AMMRC TR 78-51

LEVEL

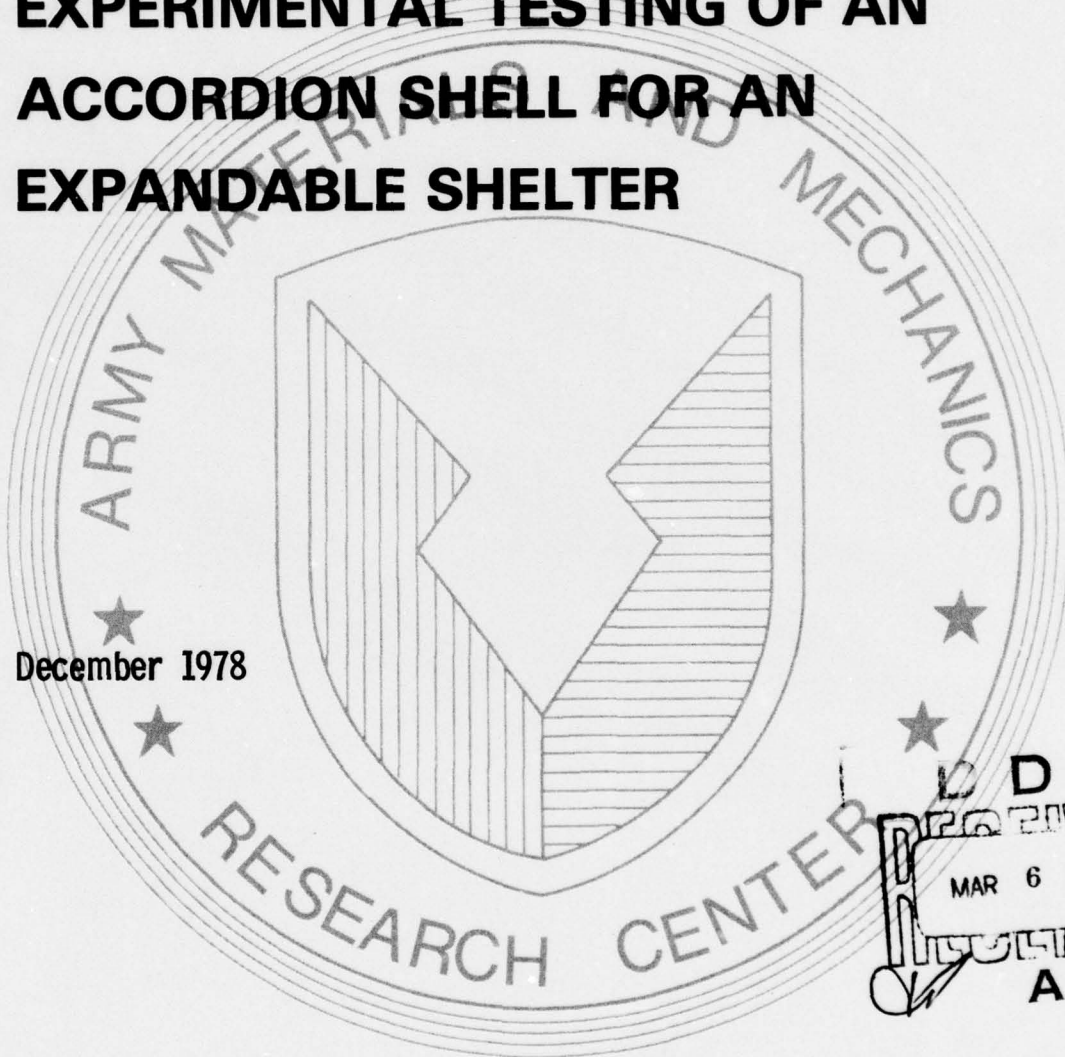# EXPERIMENTAL TESTING OF AN ACCORDION SHELL FOR AN EXPANDABLE SHELTER

December 1978

ARMY MATERIALS AND MECHANICS RESEARCH CENTER

DDC FILE COPY

AD A065264

DDC RECEIVED MAR 6 1979 A

79 03 05 088

ARMY MATERIALS AND MECHANICS RESEARCH CENTER
Watertown, Massachusetts 02172

REPORT DOCUMENTATION PAGE		READ INSTRUCTIONS BEFORE COMPLETING FORM
1. REPORT NUMBER AMMRC-TR-78-51	2. GOVT ACCESSION NO.	3. RECIPIENT'S CATALOG NUMBER
4. TITLE (and Subtitle) EXPERIMENTAL TESTING OF AN ACCORDION SHELL FOR AN EXPANDABLE SHELTER		5. TYPE OF REPORT & PERIOD COVERED Final Report
		6. PERFORMING ORG. REPORT NUMBER
7. AUTHOR(s) Robert J. Morrissey		8. CONTRACT OR GRANT NUMBER(s)
9. PERFORMING ORGANIZATION NAME AND ADDRESS Army Materials and Mechanics Research Center Watertown, Massachusetts 02172 DRXMR-T		10. PROGRAM ELEMENT, PROJECT, TASK AREA & WORK UNIT NUMBERS D/A Project: 1L162723A427 AMCMS Code: 612723.4270011 Agency Accession: DA OG4735
11. CONTROLLING OFFICE NAME AND ADDRESS U. S. Army Materiel Development and Readiness Command, Alexandria, Virginia 22333		12. REPORT DATE December 1978
		13. NUMBER OF PAGES 50
14. MONITORING AGENCY NAME & ADDRESS(if different from Controlling Office)		15. SECURITY CLASS. (of this report) Unclassified
		15a. DECLASSIFICATION/DOWNGRADING SCHEDULE

16. DISTRIBUTION STATEMENT (of this Report)

Approved for public release; distribution unlimited.

17. DISTRIBUTION STATEMENT (of the abstract entered in Block 20, if different from Report)

18. SUPPLEMENTARY NOTES

19. KEY WORDS (Continue on reverse side if necessary and identify by block number)

Shelters	Loads (forces)
Response (structural)	Deflection
Snow	Strain gages
Simulation	Strain (mechanics)

20. ABSTRACT (Continue on reverse side if necessary and identify by block number)

(SEE REVERSE SIDE)

DD FORM 1473 1 JAN 73 EDITION OF 1 NOV 65 IS OBSOLETE

Block No. 20

ABSTRACT

The Army's prototype 50-foot expandable shelter consists of a rigid shipping container measuring about 8x20 feet x 8 feet high. The two 20-foot sides, each comprised of four hinged, rigid panels, expand to form the floor and end walls of an overall 20x50-foot shelter. Each expandable section is covered by an accordion-type sandwich panel shell which serves as the roof and side walls. The goal of this project was to evaluate the capability of the shell to sustain simulated snow loading so that future shells could be designed more effectively. The snow loading was simulated by placing plywood sheets on the shell roof incrementally. Deflection and strain measurements were obtained at various specific locations on the shell roof and one side wall using several telescopic measuring devices and strain gage rosettes. These data were to be subsequently compared with an existing finite element analysis. The deflection data were basically symmetric throughout the shell and relatively linear with the loading. The strain data were generally linear with the loading, but fairly low in value. These relatively low strain values were attributed to the fact that much of the structural response action of the shell to loading took place in the shell's joints or folds.

ACCESSION for

ATIS   White Section
ODC   Buff Section
UNANNOUNCED
JUSTIFICATION

BY
DISTRIBUTION/AVAILABILITY CODES

Dist.   AVAIL. and/or SPECIAL

A

CONTENTS

INTRODUCTION

Background

In recent years the Army has been developing and evaluating a family of standardized shelters. The largest member of this family is a 50-foot expandable type of which only two prototypes exist. In its shipping condition, this shelter consists of a rigid-wall container, built to International Standards Organization (ISO) specifications, housing various shelter components and equipment. The container measures approximately 8x20 feet x 8 feet high and weighs about 8500 pounds. The two 20-foot sides, each comprised of four hinged, rigid panels, expand to form the floor and end walls of an overall 20x50-foot shelter. The panels have a paper honeycomb core impregnated with resin and faced with aluminum sheets; the floor is supported on detachable I-beams and leveling jacks. Two accordion-type shells serve as the roof and side walls for the expandable sections; these are unfolded and fastened to the container, floor, and end walls. Figure 1 is a photograph of the shelter in its fully expanded condition. Figure 2 depicts the sequence for erecting one section of the shelter. The details for erecting and stricking the shelter are provided in a technical manual prepared by Brunswick Corporation.[1]
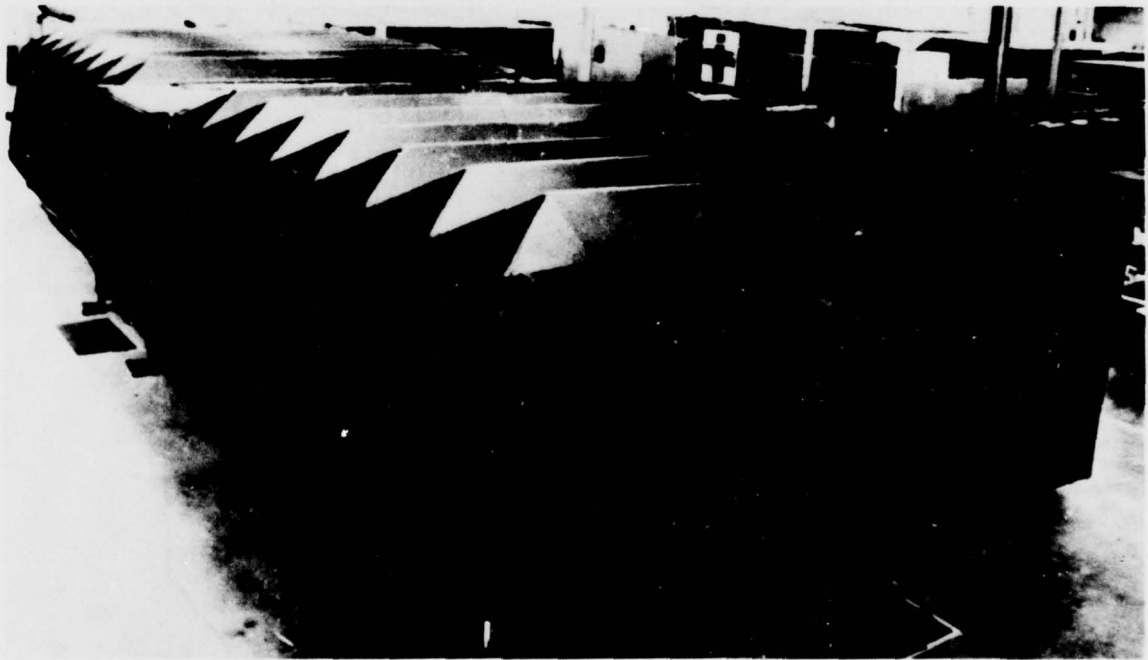

Figure 1. Fifty-foot expandable shelter.

1. *Handbook Operations and Service Instructions for U.S. Army 50' Expandable Shelter.* Brunswick Corporation, Contract DAAG17-73-C-0249, U.S. Army Natick Research and Development Command, 1 June 1976.
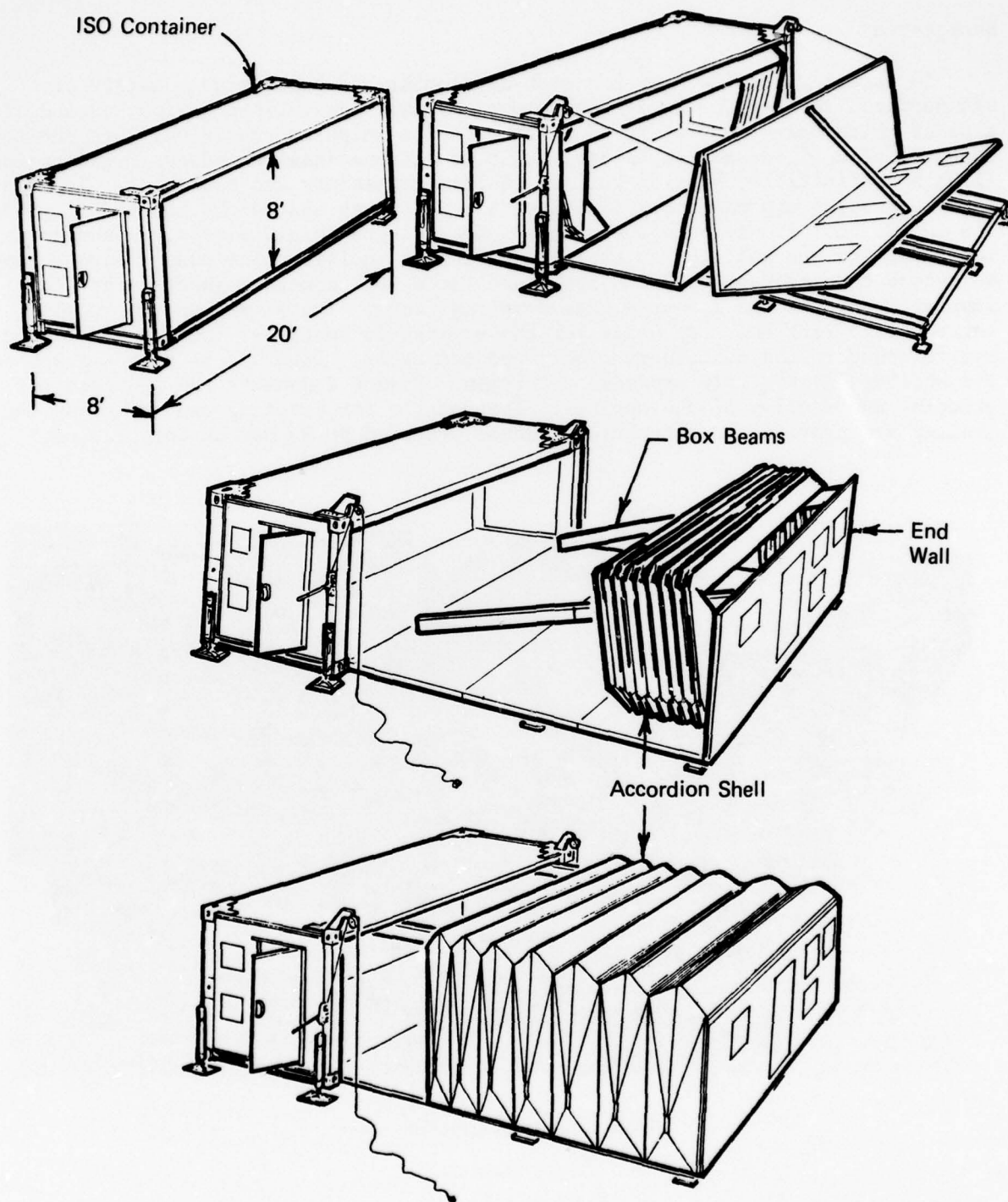
1

ISO Container

8'

20'

8'

Box Beams

End Wall

Accordion Shell

Figure 2. Sequence of erecting one side of the shelter.

2

Testing Conditions

The experimental data obtained in this investigation are to be compared with an existing Army Natick Research and Development Command (NARADCOM) finite element analysis of the accordion shell,[2] in which a two-dimensional membrane element was chosen to analyze the roof panels. There are two box beams which normally attach to the container and end wall and support the accordion shell roof. In the finite element analysis, three conditions were considered at the roof beam locations: that these beams were assumed to provide no support, elastic support, and rigid support to the shell. It is the first consideration, whereby the beams are assumed to provide no support to the shell, that is pertinent to this investigation. As specified by NARADCOM, the current tests were performed without the box beams supporting the shell roof. It should be noted that this resulted in testing the shell structure *alone* and that this loading does not correspond to service loading of the shelter itself with the box beams normally positioned to support the shell roof.

Details on the Accordion-Type Shell

The accordion shell configuration was fabricated,[3] using existing insulation manufacturing machinery, from 0.060-inch-thick foam sandwich panels, which were steel-faced with a 3-mil embossed foil, laminated to a Tedlar protective film. This machinery limited the maximum panel size that would be fabricated to about 30 inches wide by 30 feet long. These panels were joined together, resulting in the creation of fabrication joints as illustrated in Figure 3. The basic advantages of the accordion shell are its light weight, low cost, and ease of manufacture.[3]
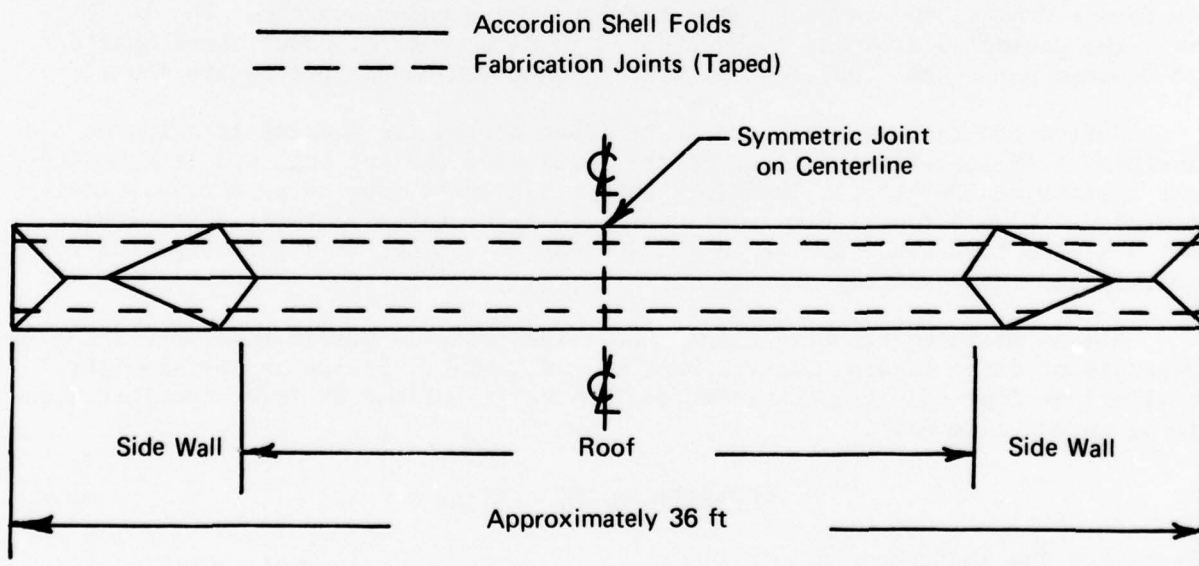
Figure 3. Schematic layout showing typical fabrication joints of accordion shell bay.

2. JOHNSON, A. *Finite Element Analysis of the Accordion Shelter Shell.* U.S. Army Natick Research and Development Command, Unpublished Technical Report, November 1976.
3. NIEDERMAYR, J., WERKEMA, M., and WITHEROW, R. *Development of Glass Fiber Reinforced Foamboard.* Sheldahl, Inc., Contract DAAG17-73-C-0236, Final Report, June 1973-February 1975, U. S. Army Natick Research and Development Command, NARADCOM TR 76-4-AMEL, February 1975.

Previous Field Testing

The prototype shelter tested in this investigation had been extensively field tested[4] (but not structurally) prior to the current experiments to examine the suitability and the potential of the shelter for military field applications. The accordion shell tested in this study was damaged during that prior field testing:[4]

"The most serious damage was shell fatigue. The damage occurred at the apex of four upper knees (folds) in one shell and three upper knees in the other shell. Damage consisted of 1- and 2-inch separations in the metal covering on both sides of the knees which worsened each time the shelter was expanded or contracted."

Much of the damage which occurred during the field testing was readily repairable by field test personnel. Nevertheless, there was still evidence of damage and/or repaired damage (i.e., punctures in shell panel, repair patches, split knee joints, and many broken or missing fasteners) at the start of the current investigation.

OBJECTIVES

The overall objective of this study as specified by NARADCOM was to experimentally test the accordion shell without it being supported (as it normally is) by the two box beams, as the shell roof was loaded with simulated snow loading. A collapse prevention support was to be installed to prevent the shell from being seriously damaged due to gross structural collapse under loading. The loading over the projected area was to be applied in increments of about three-quarters of a pound per square foot, to a total of about ten pounds per square foot.

Deflection measurements were to be taken during the loading from inside the shelter at 15 specific locations on the shell roof (or ceiling) and from outside the shelter at 12 specific locations on one side wall (due to symmetry). Additionally, these deflection measurements were to be taken in three directions - not a simple task since another objective was to conduct this investigation rather quickly and inexpensively.

Strain measurements were also to be taken using 14 strain gage rosettes (42 channels of data) located back-to-back in pairs (i.e., inside and outside the shelter) at four specific locations on the shell roof and at three specific locations on one side wall.

## PREPARATIONS FOR TESTING

Preparing the Shelter

The shelter was transported to the Army Materials and Mechanics Research Center (AMMRC) in Watertown, Massachusetts. It was set up on a platen within a

---

4. ALEXANDER, C. L. *Fifty-Foot Expandable ISO Shelter.* TRADOC Combined Arms Test Activity, Test Report FM 302, 14 September 1976.

4

large building and since the shelter is symmetric about the container, only one expandable side was erected for testing. In erecting the side, it became obvious that the fit between the accordion shell and its attachment all around to the container, floor, and end wall was a tight one. That is, we had to continuously tug, push, and pull the accordion shell to align fasteners properly, so that they could be fastened. Moreover, many of the fasteners normally used for this attachment were either damaged or missing, probably as a result of the prior field testing. We therefore made these attachments by drilling holes and inserting sheet metal screws at intervals of about one foot along these interfaces. (The screws used for attaching the shell to the floor generally worked satisfactorily.)

There are two box beams which, in their normal position (see Figure 2), transfer much of the roof loads through the container and end wall. They represent a redundant load path with the side walls to transfer roof loads to ground. If the beams are not in their normal position, the side walls are more highly loaded. One of these beams is shown in its normal position in Figure 4. Each box beam consists of two equal lengths of hollow metal box-like construction, joined together with a double pinned joint. Also shown is the top of the data logger used in obtaining strain measurements.

It was specified to observe how the shell would respond structurally to simulated snow loading without the support of these box beams. However, we did not want the shell to grossly collapse under loading because the shelter was to be subsequently used by NARADCOM. We therefore designed, fabricated, and installed brackets, spacers, etc., to reattach the beams to the container and end wall in a position one foot lower than normal. Photographs of one such beam installed in this lowered position are shown in Figure 5. Prior to testing, a telopost (i.e., column with adjustable height) was installed beneath the double-pinned joint of each box beam.
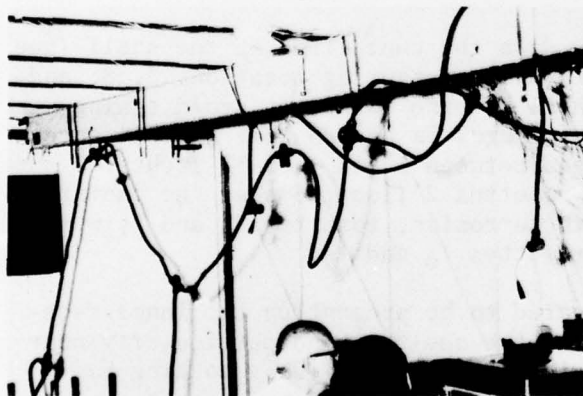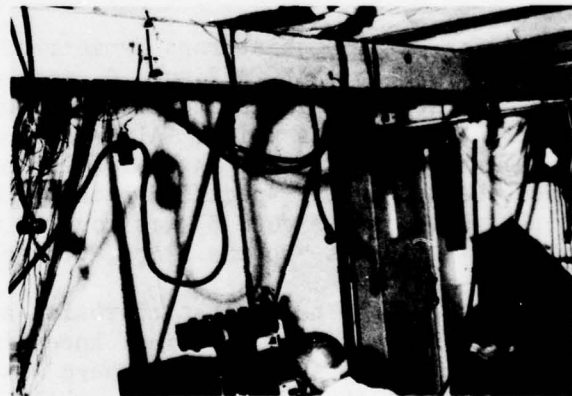
(a) End wall   (b) Container end

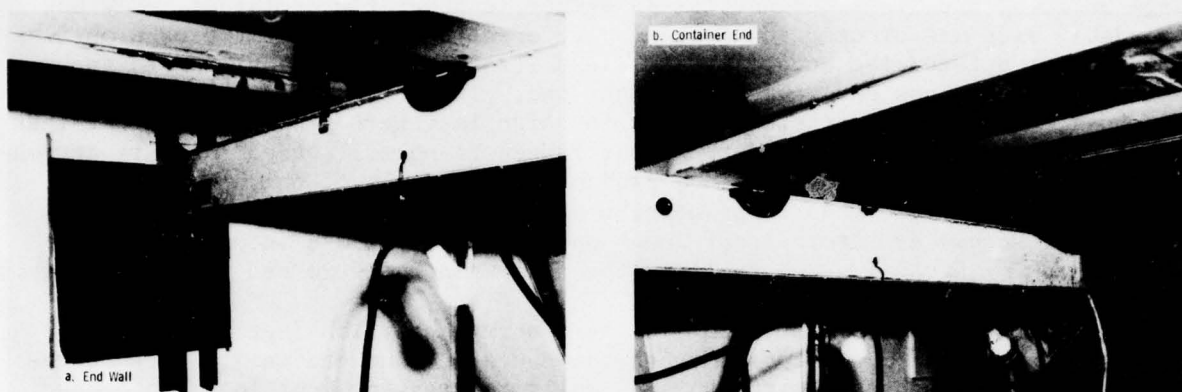Figure 4. Box beam in normal position supporting shell roof.

Figure 5. Box beam in lowered position.

Also shown in Figure 5 is part of a 2x10-inch plank which spanned and was clamped to the box beams. This was used as a reference plane in taking roof deflection measurements. There were three such planks installed beneath roof deflection points 1 through 5, 6 through 10, and 11 through 15 (see Figure 6).

Measurement Stations

Figures 6, 7, and 8 show locations where measurements of deflection and strain were made. Figure 6 provides an overview of the deflection measuring and strain gage rosette locations, while Figure 7 and 8 provide additional detailed information on these locations. Figure 6 depicts two separate orthographic or orthogonal projections joined together for convenience. The upper portion of the figure represents a view of the roof looking vertically down, while the lower portion represents an elevation view of a longitudinal or side wall.

A fabrication joint runs symmetrically down the centerline of the shell (see Figure 3). Note that in Figure 6, roof deflection measuring locations 3, 8, and 13 are offset from the centerline of the shell by nine inches to avoid taking measurements at this joint. Also notice in Figures 8a and 8b that the distance between rosettes 1 and 2 is 15-1/2 inches and between 3 and 4 is 17 inches. Since the originally specified location of rosettes 2 (located near the center of the shell, see Figure 6) was covered with corrosion, rosettes 2_o and 2_i were moved 1-1/2 inches "up the slope," toward rosettes 1_o and 1_i.

It should be noted that corrosion appeared to be present on the inner face-sheets of many of the lower roof knees inside the shelter, and particularly near the center of the shell roof. There was evidence that the Tedlar coating had separated from the face-sheet along these areas. The corrosion was apparently caused by rain water or melting snow captured on the roof, eventually seeping through joints and/or punctures and through the foam core material to corrode the inner face-sheet, starting from the inner or core side of that face-sheet. We deem this a significant finding which could lead to loss of structural integrity. Figure 9 depicts this assumed cause of the inner face-sheet corrosion.

6

o = DEFLECTION MEASUREMENT LOCATION

∠ = STRAIN GAGE ROSETTE LOCATION/ORIENTATION
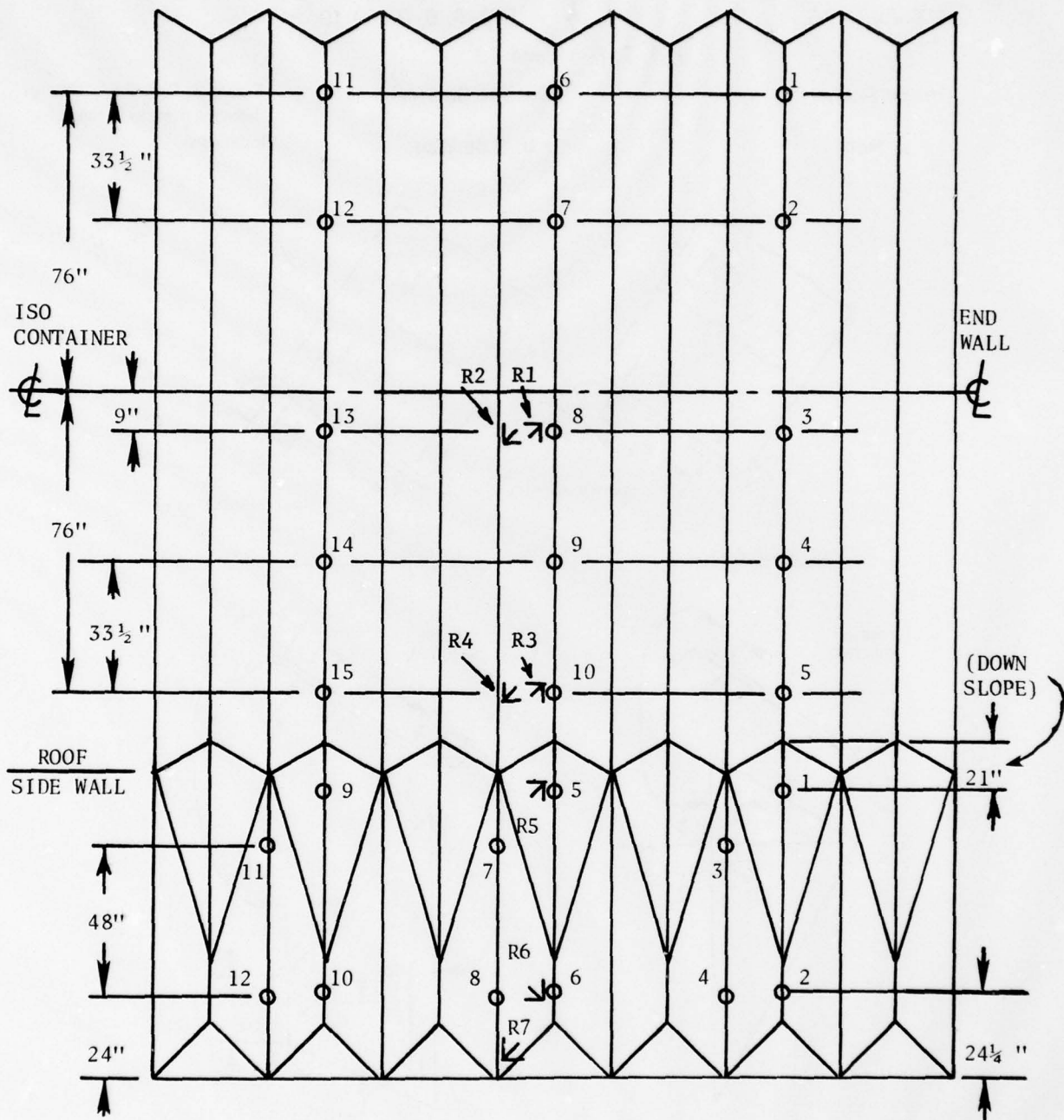
Figure 6. Orthographic projections of shell roof and wall depicting overview of
deflection measurement and strain gage rosette locations.

7

(Outside Shelter)

(Inside Shelter)

1 Through 15

1, 2, 5, 6, 9 and 10

3, 4, 7, 8, 11 and 12

(Inside Shelter)

(Outside Shelter)

a. Roof

b. Side Wall
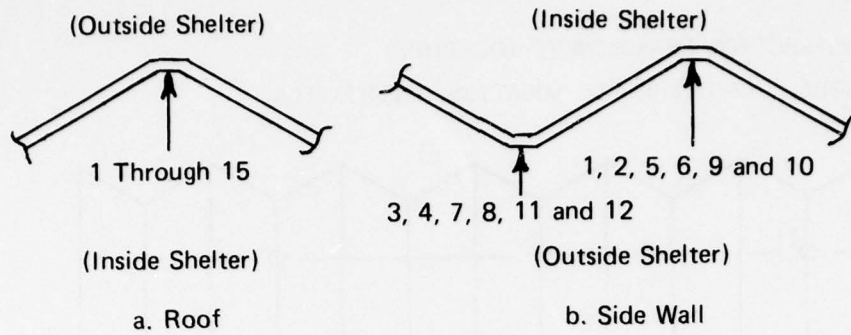
Figure 7. Schematic view of deflection measurement locations.

1_o

2_o

$1\frac{1}{2}''$

$15\frac{1}{2}''$ 1_i

2_i

(INSIDE SHELTER)

a) Rosettes 1 and 2

3_o

4_o

$1\frac{1}{2}''$

$17''$ 3_i

4_i

(INSIDE SHELTER)

b) Rosettes 3 and 4

5_i

(INSIDE SHELTER)

$1\frac{1}{2}$

5_o

$1\frac{1}{2}''$

H

$45°$ V

c) Rosettes 5

6_i

(INSIDE SHELTER)

7_i $17''$

6_o

7_o

$1\frac{1}{2}''$

$1\frac{1}{2}''$

$45°$ V

H

$11\frac{1}{2}''$

5 3/4''

V $45°$

H

$19''$

d) Rosettes 6 and 7

Figure 8. Strain gage rosette locations and orientations.

8

Figure 9. Illustration of assumed cause of corrosion of inner face-sheets of lower roof knees.

Deflection Measurement Technique

Deflection measurements were taken three-dimensionally at 27 locations on the accordion shell for each loading increment. Since 14 loading increments were planned and sin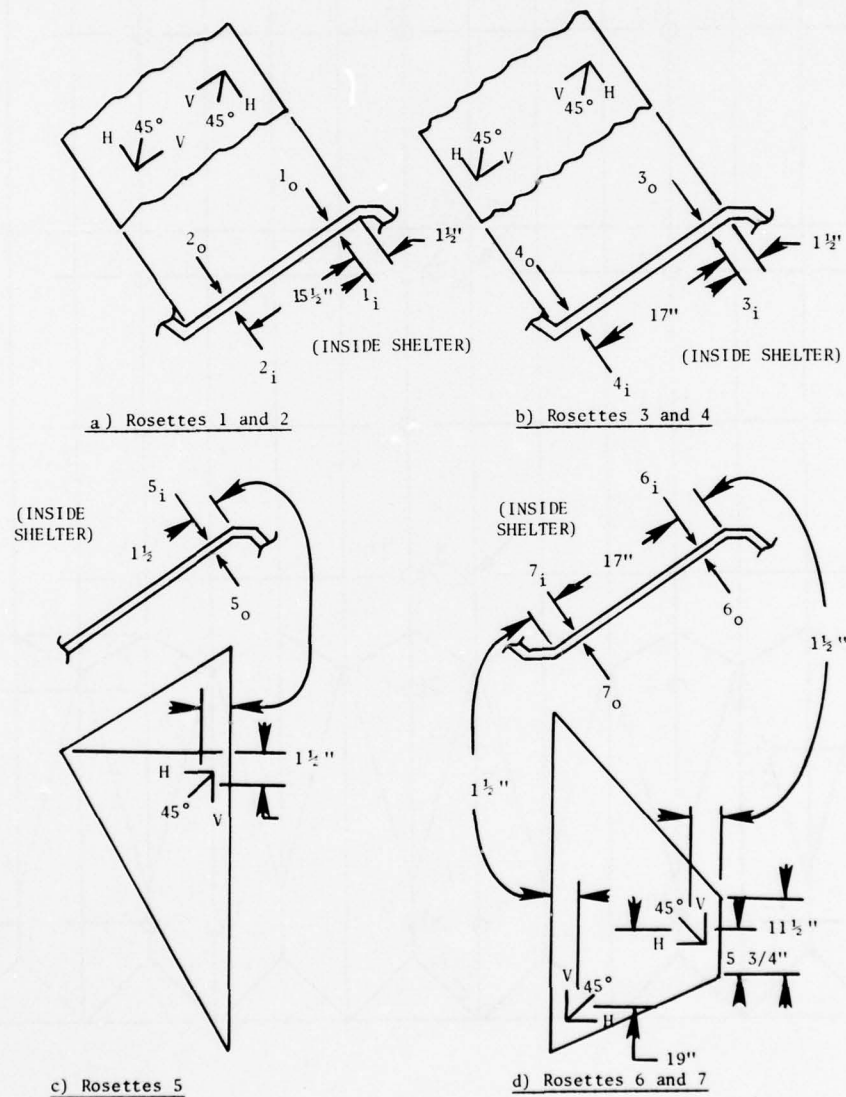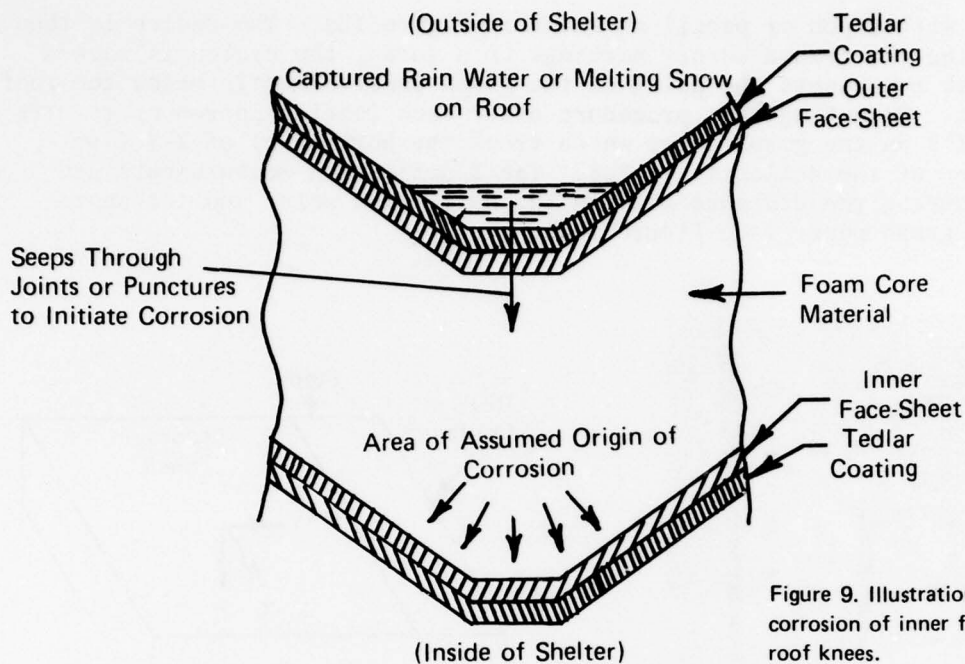ce a zero deflection reading was also necessary, 1215 deflection measurements were anticipated (i.e., 27 locations times 3 dimensions times 15 readings).

Four measuring devices, each telescopically adjustable to within a few inches, were designed and constructed (see Figure 10) to be used with a scale and reference plane to take three-dimensional deflection measurements. These devices consist of a piece of drill rod with a pointed end whose other end slides in a piece of aluminum tubing, which in turn slides in a drilled and reamed rod. The rod is centrally fastened to an 8-inch square aluminum plate. Thumb screws in both the tubing and rod permit locking the device at a particular telescopic setting. The four devices are indentical except for the difference in the length of the drill rods required because of the significant variation in the distances to be measured between the various deflection measurement locations and the reference planes. One such device was used for taking roof deflections and three for taking side wall deflections.

Figure 11 shows the sign convention used for deflection measurements and Figure 12 shows roof deflection measurements being taken. The appropriate telescopic device is placed on a graph paper which is taped to the upper surface of the reference plank below a roof deflection location. The device is moved and adjusted until the pointed end of the drill rod is just touching a marked deflection point. The four corners of the base plate of the device are then traced on

9

the graph paper with a pen or pencil as shown in Figure 12a. The device is then removed. By using the traced corner markings as a guide, the center is marked with an "X" which represents the point on the graph paper directly below the roof deflection point. Repeating this procedure after each loading increment results in a series of X's on the graph paper which track the horizontal of X-Y (see Figure 11) motion of the deflection point. The Z deflection measurements are obtained by measuring the distance between the deflection point and the appropriate X on the graph paper (see Figure 12b).
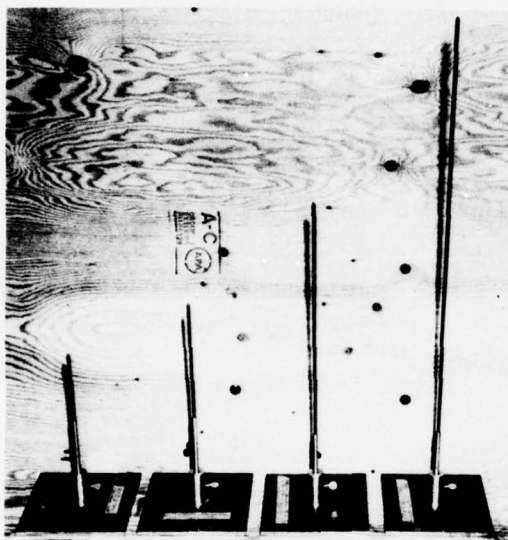
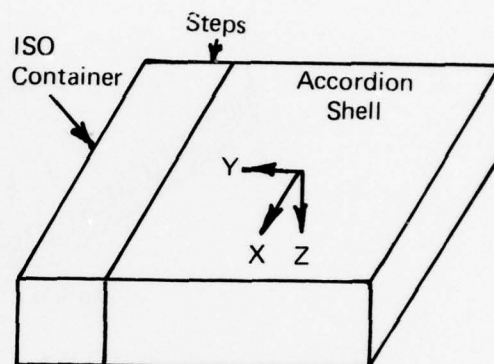

Figure 10. Telescopic deflection measuring devices.

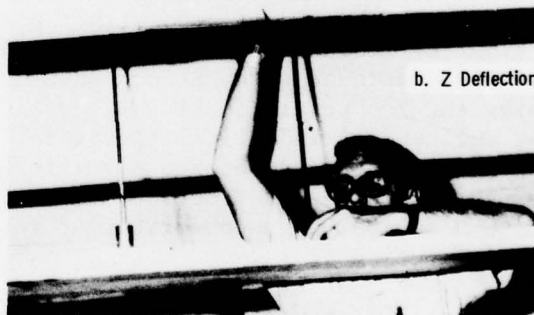Figure 11. Sketch showing sign convention for deflection measurements.

Figure 12. Roof deflection measurements being taken.

10

A wooden reference "wall," shown in Figure 13, was constructed for taking side wall deflection measurements. Figures 14a and 14b show side wall deflection measurements being taken using the shortest telescopic device. In taking these measurements, the Y and Z deflections (see Figure 11) were tracked on the graph paper and the X deflection was read from a scale.

A pencil or pen color code was employed to identify loading increments in tracking deflections on the graph paper. These plots were subsequently scaled directly to obtain deflection measurements.

Strain Measurement Technique

Strain measurements were taken using 14 strain gage rosettes (42 channels of data) located back-to-back, in pairs, at 4 locations on the roof and at 3 locations on one side wall. The rosettes installed were BLH type FAER-25R-12-S6. These gages were installed by carefully scraping off the Tedlar coating with a knife within a 1-1/4-inch circle and then applying the gages in a routine fashion. Figure 15a, a photograph of rosette 3_i, also shows roof deflection point 10 above and lead wires from rosettes 3_o and 4_o entering the shelter through a hole drilled through the shell below.

Figure 15b is a close-up photograph of rosette 5_i which shows the embossed hills on the face-sheet. Since these hills are of the same order of magnitude as the gages, the strain data may contain some surface effects associated with the hills which is not representative of the gross structural behavior of the shell.

The rosettes were wired into a 48-channel data logger which provided output in terms of millivolts. The millivolt data were to be converted to strain data via the standard formula:

$$\varepsilon = E_o/KV \ (N/4)$$

where

ε = strain in microinches per inch
E_o = data logger reading in millivolts
K = strain gage factor (1.98)
V = excitation voltage of bridge in millivolts (1401)
N = number of active gages (1).

Simulation of Snow Loading

"Weather bureau records show that about 90 percent of all snowfall occurs at temperatures between 10 and 35 F or at an average temperature of 26 F. At 26 F the average density of snow is 6 lb per cu ft."[5] Various methods were considered for the simulation of snow loading before adopting the use of plywood sheets. (It was noted that actual snow loading would initially concentrate in the valleys between the roof ridges, whereas simulated snow loading with plywood sheets would concentrate the loading on the ridges and possibly cause localized crippling. A preliminary test was therefore performed on an available section of a shell roof

5. *Marks' Standard Handbook for Mechanical Engineers.* McGraw-Hill Book Company, New York, 1967, Seventh Edition, p. 12-108.
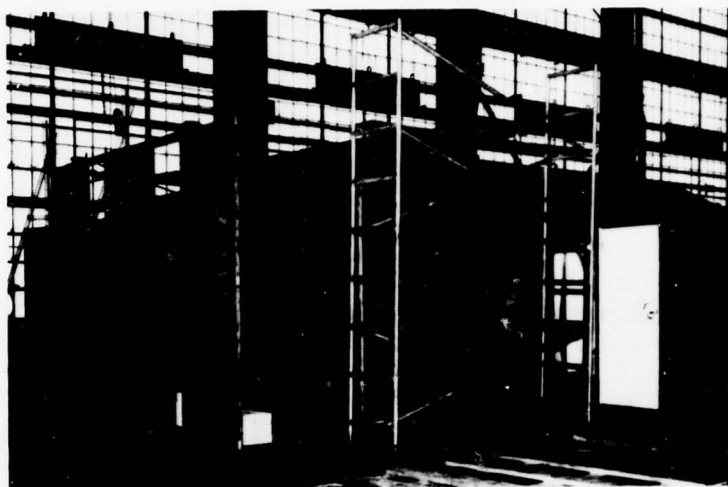
Figure 13. View showing shelter, wooden reference "wall" for the side wall deflection measurements and staging supporting ladder used in loading shell roof.

a. Y-Z Deflections

b. X Deflections

Figure 14. Side wall deflection measurements being taken.
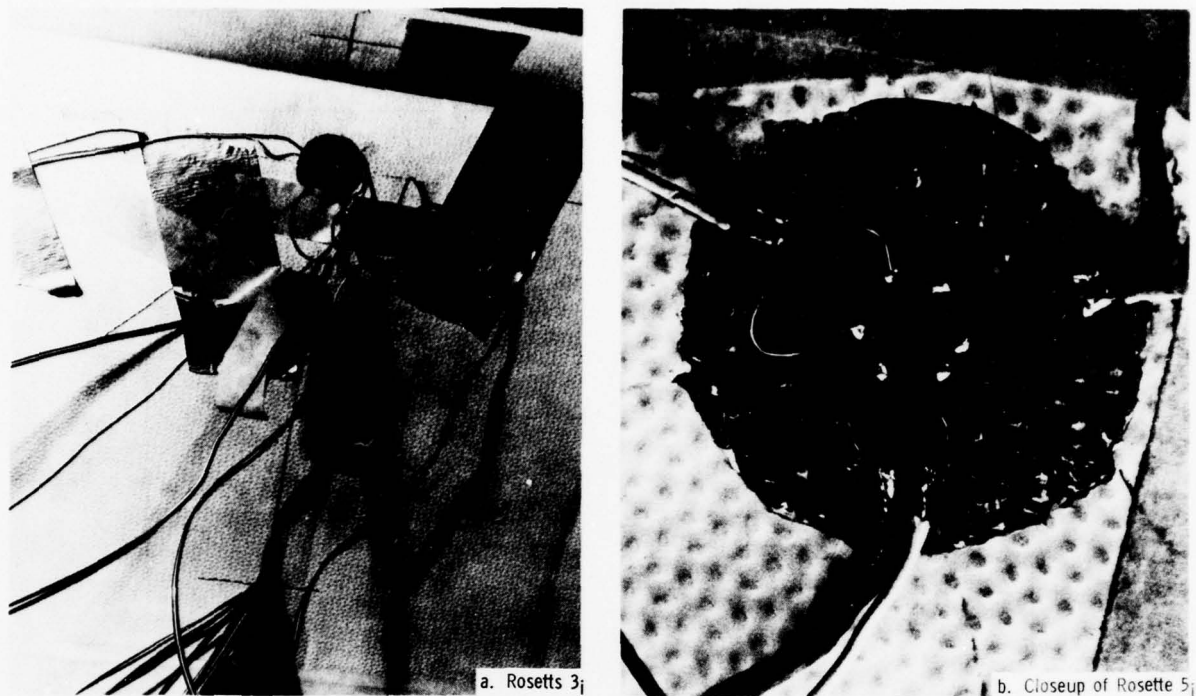
a. Rosetts 3;   b. Closeup of Rosette 5;

Figure 15. Photographs of strain gage rosettes.

bay and no localized crippling effects were observed. The details of this test are discussed in Appendix A.) Figure 16 is an illustration of the simulated snow loading technique used in this investigation. A projected area of 388.5 square feet was selected which is the actual floor area, 21x18-1/2 feet. Notice that the accordion shell has seven bays, each 3x18-1/2 feet (55.5 square feet). Each loading increment would consist of eight sheets of 4x8-foot plywood: four sheets of 3/8-inch-thick plywood for the middle three bays, two sheets of 1/2-inch-thick plywood for each of the two end bays. The different thicknesses of plywood were planned to achieve a more uniform loading over the total projected area. The four end bays have one-third greater projected area than the three middle bays. Therefore, the 1/2-inch-thick plywood used for the end bays was one-third thicker than the 3/8-inch-thick plywood used for the middle bays.

In addition, the plywood sheets used to load the middle bays were sawed into 2x8-foot sheets to facilitate loading/unloading them from the ladder walkway. The less pliable 1/2-inch-thick plywood used for the first two loading increments on the end sections was cut into 2x4-foot sheets to achieve a more uniform load over the end bays.

The plywood sheets were sawed, as necessary, and then weighed in terms of loading increments for the middle section, and for both end sections taken together. These weights were recorded and the plywood was stacked by loading increments.

13
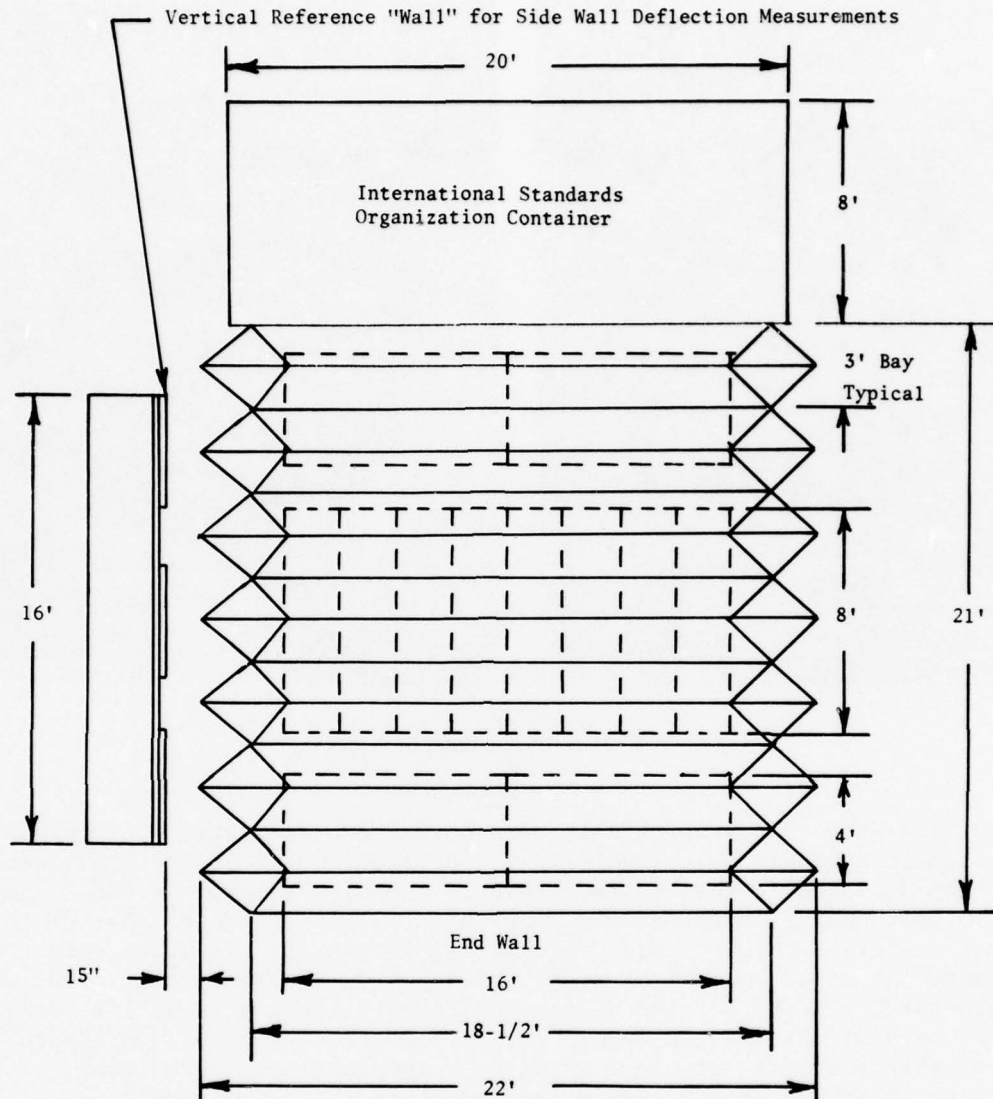
Figure 16. Pattern for positioning plywood sheets on shell roof for simulation of snow loading.

Figure 17 is a plot of the planned simulated snow loading of the shell roof. The data for this plot is contained in Table 1, both incrementally and cumulatively. The average planned increment of load in terms of pounds per square foot over the projected area was 0.738 for the middle section, 0.753 for both end sections taken together, and 0.746 over the total area. Table 2 shows the variation from uniform accumulative loading using the data presented in Table 1. Table 2 also shows that the planned loading was uniform over the total projected area to within a few percent.

14

Figure 17. Planned accumulative loading over projected areas.

Table 1. SIMULATED SNOW LOADING OF ACCORDION SHELL ROOF

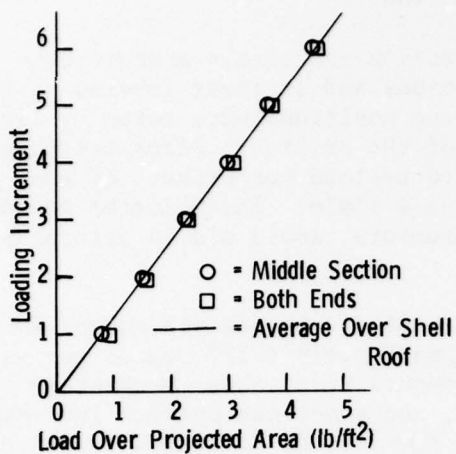| (Projected Area) →	(166.5 ft²)		(222 ft²)		(388.5 ft²)	
Loading Increment	Middle Section* lb	lb/ft²	Both Ends† lb	lb/ft²	Average Over Total Roof lb	lb/ft²
1	123.4	0.741	173.9	0.783	297.3	0.765
2	119.9	.720	161.9	.729	281.8	.725
3	123.0	.739	166.4	.749	289.5	.745
4	125.1	.751	166.0	.748	291.1	.749
5	120.3	.723	166.3	.749	286.6	.738
6	125.4	.753	168.3	.758	293.7	.756
Average	122.8	0.738	167.1	0.753	290.0	0.746
Cumulative 1	123.4	0.741	173.9	0.783	297.3	0.765
Loading 2	243.3	1.461	335.8	1.513	589.1	1.491
Totals 3	366.3	2.000	502.2	2.262	868.5	2.235
4	491.4	2.951	668.2	3.010	1159.6	2.985
5	611.7	3.674	834.5	3.759	1446.2	3.722
6	737.1	4.427	1002.8	4.517	1739.9	4.478

*All loading increments were 2x8-foot pieces of plywood, 3/8 inch thick.
†First two loading increments were 2x4-foot pieces of plywood, 1/2 inch thick. Subsequent increments were 4x8-foot sheets of plywood, 1/2 inch thick.

Table 2. PERCENT VARIATION* IN SIMULATED SNOW LOADING COMPARED TO ACCUMULATIVE AVERAGE OVER TOTAL PROJECTED AREA

Loading Increment	Middle Section, %	Both Ends, %
1	-3.1	+2.4
2	-2.0	+1.5
3	-1.6	+1.2
4	-1.1	+0.8
5	-1.3	+1.0
6	-1.1	+0.8

*+ and - mean greater or less than the accumulative average over both the middle section and both end sections, all taken together.

15

TESTING

Prior to testing, two no-load deflection and strain measurements were taken with the box beams in their normal positions and in their lowered positions. The roof deflection measurements for both beam positions were taken by expanding a measuring tape vertically to the floor of the shelter. After the planks were clamped in position to the beams, a third no-load measurement of roof deflections was taken with the telescopic devices and a scale. These latter measurements, along with initial and subsequent measurements, would aid in determining accumulative roof deflections.

Six incremental loadings, each of about 3/4 pounds per square foot, were applied for an accumulative total of approximately 4-1/2 pounds per square foot over the projected area. Strain measurements were taken immediately before and immediately after each incremental load, and sometimes between increments as a balance or creep check. It took only a few seconds to record strain data via the data logger for a given loading increment, whereas it took between 1/2 hour to an hour to take and record both roof and side wall deflection measurements.

As anticipated, the largest deflections occurred at roof deflection point 8 (located nearest the center of the roof) in the vertically downward direction. This deflection measurement will be used during the following discussion as a general guide as to how the shell roof behaved structurally under loading.

As a consequence of lowering the box beams, the shell roof deflected vertically downward somewhat, but not perceptibly in the horizontal directions. Six increments of loading were applied to the shell roof over a period of 1-1/2 days. Figure 18 is a photograph of the shell roof after the first loading increment was applied. There was concern during the loading that the accordion shell might buckle or collapse in a gross structural manner, particularly along the symmetric fabrication joint. Therefore, after the third loading increment had been applied a collapse prevention support was built along this joint, beneath the center of the shell roof.

After the fourth loading increment was applied, the accordion shell began to fail structurally. There were wrinkles on the interior skin of the roof and side walls, misalignment of the symmetric fabrication joint, and crushing of the bases of some of the interbay columns of the side walls. These signs of failure became more pronounced as additional loading increments were applied. Figure 19 shows the exterior of the shelter after the sixth loading increment was applied. Since the sixth loading increment was applied late in a working day, deflection measurements were not taken immediately, but delayed purposely until the next morning so that such measurements would include any overnight creep. Overnight the shell roof settled on the collapse prevention supports. The central portion of the shell roof was raised by hand and the collapse prevention supports were adjusted so that the shell roof was again free to deflect naturally. Deflection measurements were taken then and again 1-1/2 hours later. Table 3 shows the vertically downward deflections of roof deflection point 8 throughout the testing.

During the creep period just mentioned, some of the taped exterior joints of the side wall popped audibly, splitting open from the stress. It was apparent
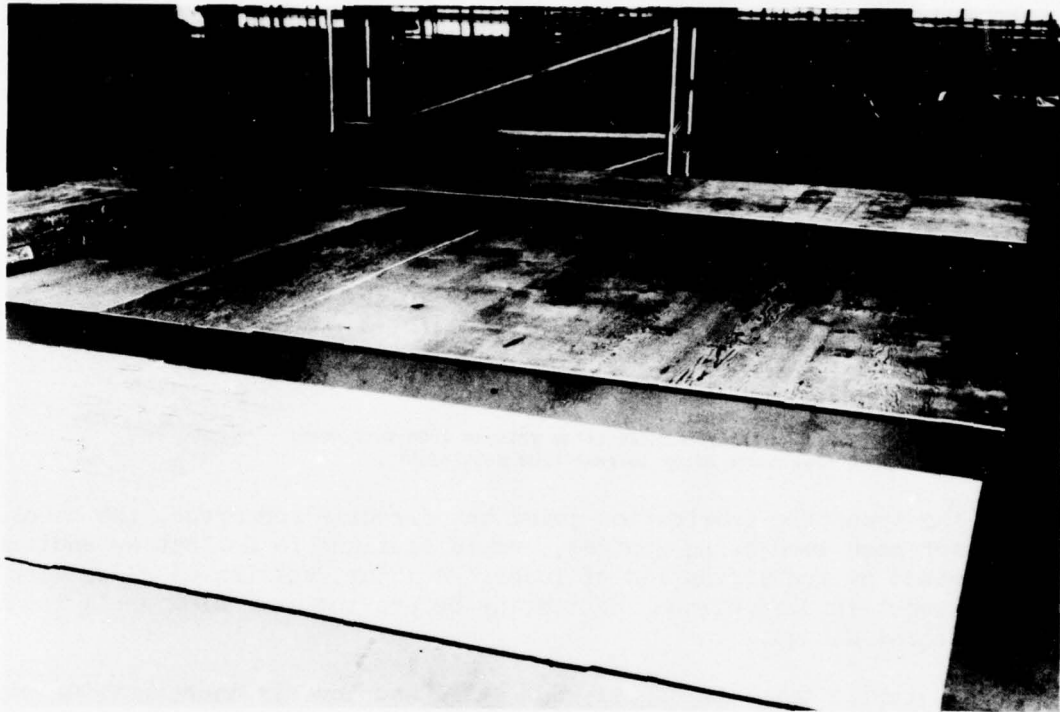
16

Figure 18. View of shell roof after first loading increment was applied.
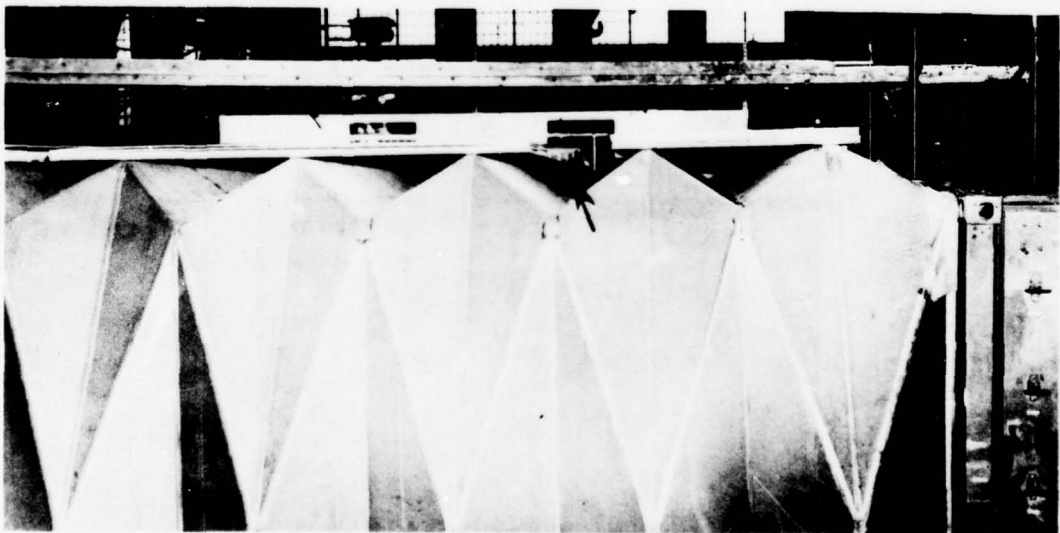

Figure 19. Exterior side view photograph of shelter showing plywood sheets loading
on accordion shell roof after sixth loading increment was applied.

17

Table 3. VERTICALLY DOWNWARD DEFLECTION OF ROOF DEFLECTION POINT 8

| Loading Condition | Deflection (inches) | |
	Incremental	Accumulative
0_a (beams normally positioned)	0	0
0_b (beams lowered)	1/4	1/4
1	1/2	3/4
2	5/16	1-1/16
3	3/8	1-7/16
4	1-5/16	2-3/4
5	1/2	3-1/4
6	1-1/4	4-1/2
6*	3/8	4-7/8
6†	5/16	5-3/16
6‡	1/4	5-7/16
6**	1/8	5-9/16

*After overnight settlement
†Twenty minutes later
‡One hour and forty minutes after release from settlement
**About four hours after release from settlement

that unless the symmetric fabrication joint was directly supported, the accordion shell - without more load being applied - would continue to deflect as additional damage was caused by redistribution of loads. A joint decision was made with NARADCOM personnel to discontinue the testing before the accordion shell incurred further structural damage.

At this point in time, the shell roof still had the six increments of plywood sheet on it, weighing a total of 1,739.9 pounds or equivalent to an average load of 4.478 pounds per square foot over the projected area (see Table 1). Photographs were taken to show some of the characteristics of the structural failure behavior of the accordion shell. In the captions of these photographs, the reference to left or right refers to the shelter as depicted in Figure 16.

Figure 20 shows a severely damaged corner (about a seven-inch-long split) at the top of the first interbay column from the container on the right side wall. Figures 21 and 22 show interior and exterior views of crushed and uncrushed interbay columns of the side wall.

Figure 20. Split corner at top of the first interbay column from the container on the right side wall.
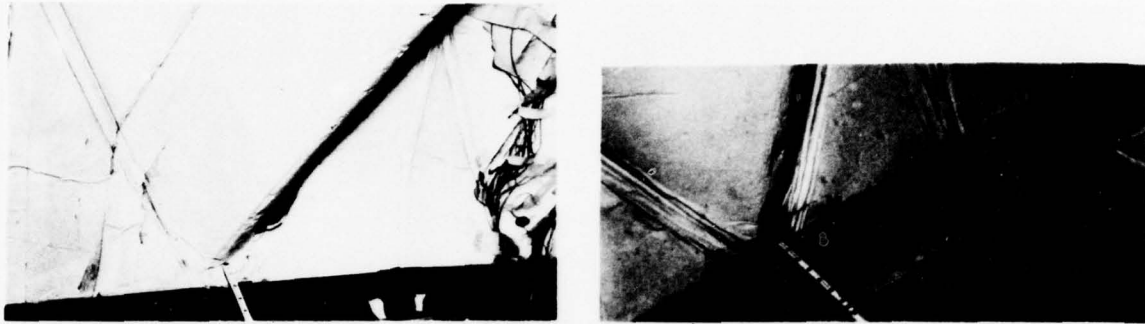
18

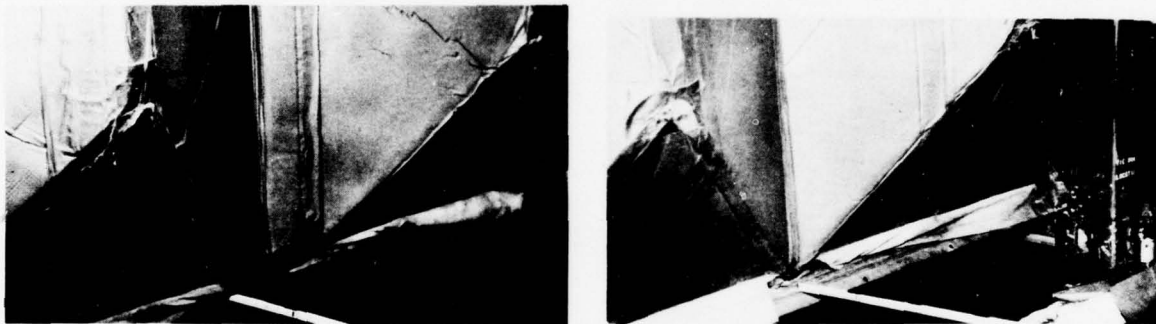Figure 21. Interior view of crushed and uncrushed interbay column bases.

Figure 22. Exterior view of crushed and uncrushed interbay column bases.

Figure 23 includes a photograph taken from inside the shelter from the left hand side of the symmetric fabrication joint, showing the misalignment of the shell sandwich panel along this joint due to out-of-plane shearing action, and a sketch depicting this action. Part of the collapse prevention support is shown in the right foreground. For comparison purposes, the upper left of Figure 12a shows similar undamaged joints taken from a different camera angle at about the time the second loading increment was applied.

Figure 24 is a photograph taken from inside the shelter of the second inter-bay column from the end wall on the left side wall, showing the skin wrinkling and delamination characteristics which were generally present on the inside of the side wall bays. Some skin wrinkling was also visible on the exterior sur-faces of the side walls (see Figure 22). Figure 25 is a sketch made of the in-terior view of the left side wall showing skin wrinkling patterns. Many of these wrinkles started or ended at the location of fabrication joints.

The original plan for this investigation did not specify taking strain or deflection measurements during unloading. However, since they were so easy to obtain, strain measurements were taken incrementally during manual unloading; deflection values were not accumulated because of the much longer times required to make these measurements.
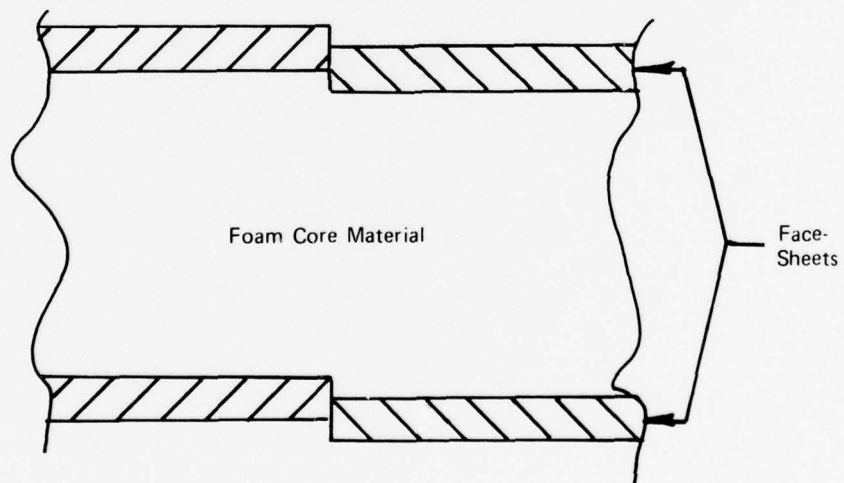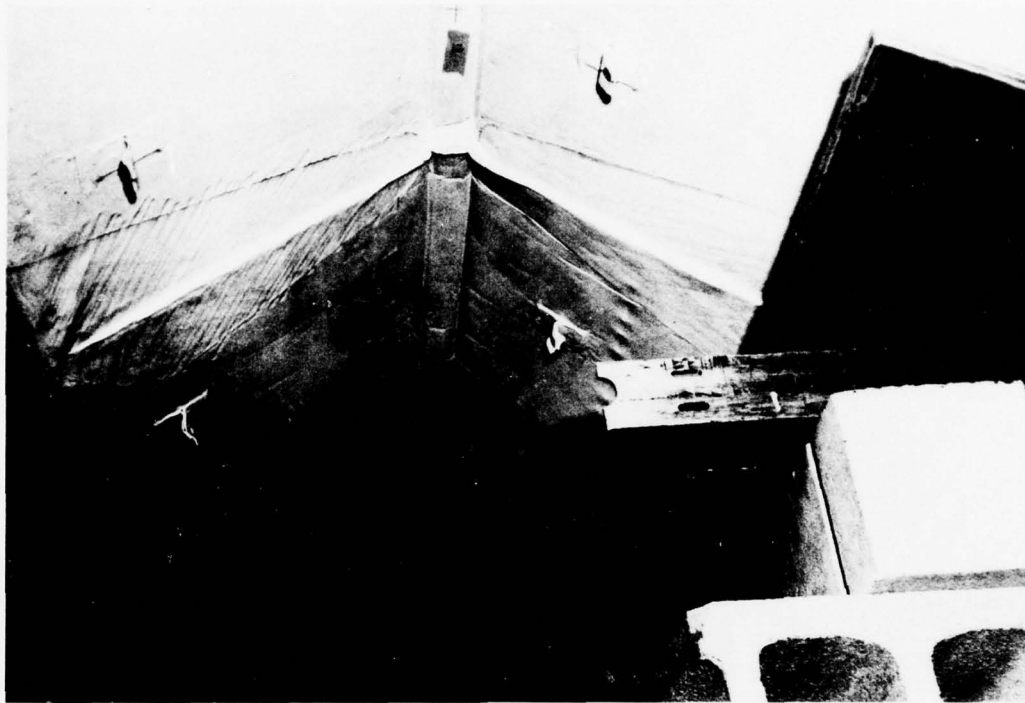
19

Figure 23. Misalignment of fabrication joint due to out-of-plane shearing action.
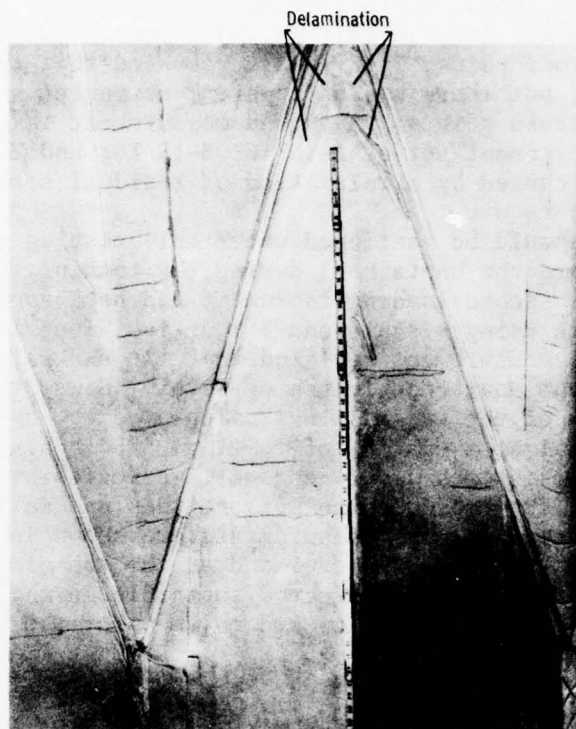
Figure 24. Skin wrinkling and delamination on the inside
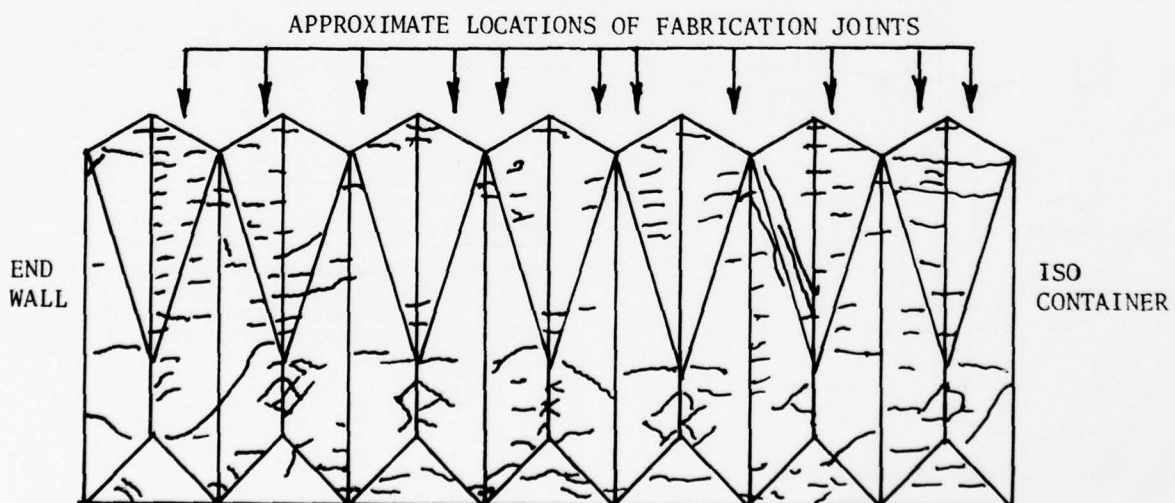of the left side wall at the second bay from the end wall.

Figure 25. Sketch of skin wrinkle patterns on left side wall as viewed from inside shelter.

21

After unloading the shell, the box beams were detached, raised one foot, and reattached to the container and end wall in their normal position. Deflection measurements taken at roof points 7, 8, and 9 revealed that the roof did not rise to its original height, but there was an apparent permanent set of 3-3/16, 3-9/16, and 2-15/16 inches at these points. A second measurement taken 11 days later revealed an apparent permanent set of 2-10/16, 3-15/16, and 2-12/16 inches. This reduction was probably caused by a relaxation of residual stresses in the shell.

One final aspect should be mentioned under this testing section. The end wall moved inward (toward the container) during the testing. This movement was first noticed after the second loading increment had been applied. We measured this movement henceforth using a scale and a four-foot-long level as depicted in Figure 26. The initial measurement revealed that the end wall was 3/8 inch from being vertical - over the four-foot length of level. Since the end wall was about 80 inches high, the top of the end wall was calculated to have moved inward (assuming it was vertical at the start of testing) 5/8 inch. Similarly, the point where the box beams attach to the end wall was calculated to have moved inward by about 1/2 inch. We continued to measure this end wall measurement throughout the rest of the testing. These measurements are shown in Table 4 along with the calculated movements at box beam level and at the top of the end wall. There did not appear to be any pronounced effect discernible in the deflection data which was clearly attributable to the inward movement of the end wall or box beams.
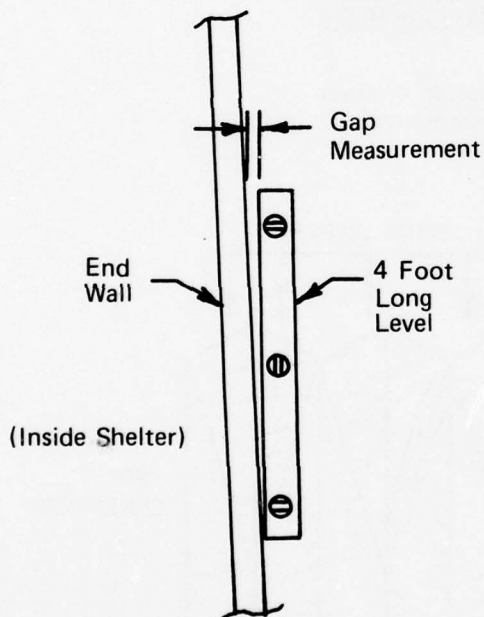
Figure 26. Sketch of how end wall movement was measured.

Table 4. END WALL MOVEMENT MEASUREMENTS AND CALCULATED MOVEMENTS
(In Sixteenths of an Inch)

Loading Increment	Measured Gap	At Box Beam Level	At Top of End Wall
2	6	8	10
3	11	15	18.5
4	11	15	18.5
5	11	15	18.5
6*	11	15	18.5
6**	10.5	14	17.5
Unloaded	10	13.5	16.6

*After roof of accordion had settled overnight on to the collapse prevention supports.
**An hour and a half after collapse prevention supports were adjusted such that the roof could deflect naturally.

22

TEST RESULTS

Roof Deflection Measurements

The deflection measurements for the fifteen roof deflection locations (see Figure 6) in each of the three directions (X, Y, and Z) are presented in Table 5.* A sketch of Figure 11 is also shown in that table to facilitate understanding the signs of the deflection measurements. The deflection directions will be shown with arrows on all plots or tables of roof and side wall deflection measurements. In addition, 0_a, 0_b, 6*, and 6** appear as loading increments on many of these plots or tables. The no-load deflection measurements were taken with the box beams normally positioned (0_a) and in their lowered position (0_b). The sixth loading increment was applied late in a working day, the deflection measurements were taken the next morning so that any creep would be included in the readings. It was noted that the roof had settled on the collapse prevention structure over-night. The supports were adjusted such that the roof was free to deflect and deflection measurement 6* was taken. About 1-1/2 hours later deflection measure-ments 6** were taken.

Figure 27 is a plot of the accumulative roof deflections in the vertical (Z) direction. This figure is actually three plots (i.e., deflection of points 1-5, 6-10, and 11-15) shown together to facilitate comparison of the data. (Figures 6 and 7 can be referred to for identification of the location of these roof de-flection points.) The symmetry of the data plotted in this figure is obvious.
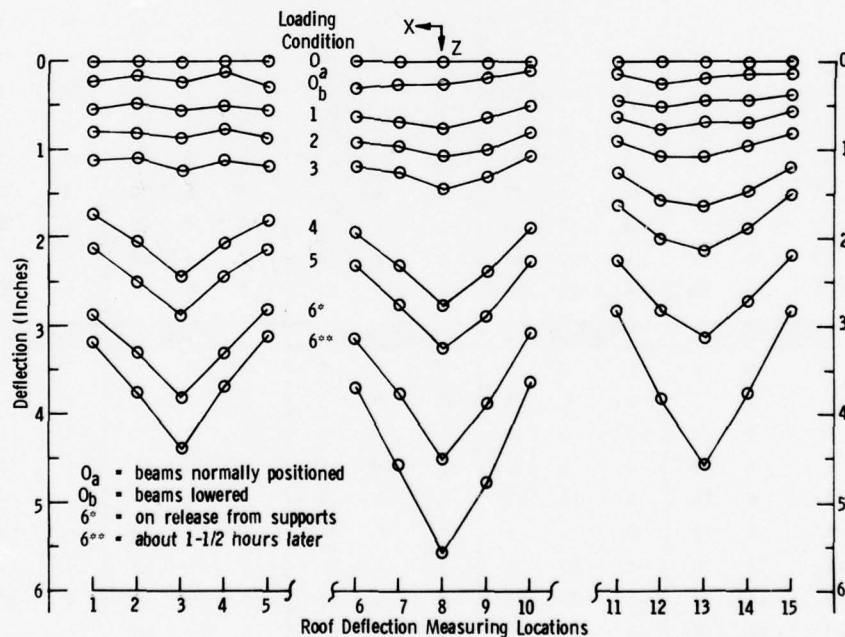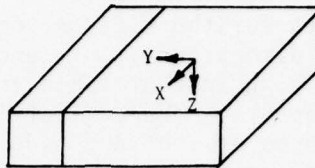

Figure 27. Accumulative roof deflections in the vertical (z) direction plotted by rows in the X-direction.

*All deflection measurements were recorded in terms of sixteenths of an inch, being read either directly from a scale or scaled off the graph paper plots.

23

Table 5. ROOF DEFLECTION MEASUREMENTS
(In Sixteenths of an Inch)

Loading Increment	X	Y	Z	X	Y	Z	X	Y	Z	X	Y	Z	X	Y	Z
	LOCATION #1			LOCATION #2			LOCATION #3			LOCATION #4			LOCATION #5		
0_a	0	0	0	0	0	0	0	0	0	0	0	0	0	0	0
0_b	0	0	4	0	0	3	0	0	4	0	0	2	0	0	5
1	0	0	9	0	0	8	0	0	9	0	0	8	0	0	9
2	-2	-7	13	-1	-1	13	0	0	14	-1	-1	12	-1	-3	14
3	0	-9	18	1	-5	18	0	-3	20	0	-4	18	-1	-5	19
4	-1	-13	28	-1	-8	33	2	-8	39	0	-8	33	0	-10	29
5	-3	-15	34	-2	-9	40	0	-7	46	0	-11	39	-1	-11	34
6*	-2	-16	46	-2	-13	53	1	-12	61	0	-13	53	-1	-15	45
6**	-2	-18	51	-3	-15	60	2	-15	70	2	-16	59	1	-17	50
	LOCATION #6			LOCATION #7			LOCATION #8			LOCATION #9			LOCATION #10		
0_a	0	0	0	0	0	0	0	0	0	0	0	0	0	0	0
0_b	0	0	5	0	0	4	0	0	4	0	0	3	0	0	2
1	-1	3	10	0	0	11	0	0	12	0	0	10	0	0	8
2	0	4	15	-1	6	15	0	0	17	0	0	16	0	0	13
3	-1	3	19	0	4	20	3	3	23	1	5	21	0	3	17
4	-1	4	31	-2	5	37	0	4	44	3	2	38	3	2	30
5	-5	5	37	-4	8	44	-1	6	52	0	6	46	2	4	36
6*	-4	9	50	-4	11	60	1	8	72	3	6	62	5	4	49
6**	-6	11	59	-6	12	73	-1	11	89	3	8	76	5	4	58
	LOCATION #11			LOCATION #12			LOCATION #13			LOCATION #14			LOCATION #15		
0_a	0	0	0	0	0	0	0	0	0	0	0	0	0	0	0
0_b	0	0	2	0	0	4	0	0	3	0	0	2	0	0	2
1	0	0	7	0	6	8	0	5	7	0	5	7	0	4	6
2	0	4	10	0	6	12	-1	8	11	0	5	11	-1	7	9
3	1	6	14	2	10	17	2	8	17	0	8	15	0	6	13
4	-1	9	20	0	9	25	0	9	26	0	9	23	1	10	19
5	-2	12	26	-1	15	32	0	14	34	0	15	30	0	14	24
6*	0	14	36	-1	20	45	1	17	50	3	19	43	4	20	35
6**	-5	17	45	-3	20	61	3	20	73	5	22	60	6	23	45

*Deflection measurements taken after freed from overnight settlement.
**Deflection measurements taken 1-1/2 hours later.

24

AD _____
    UNCLASSIFIED
UNLIMITED DISTRIBUTION

Army Materials and Mechanics Research Center,
   Watertown, Massachusetts 02172
EXPERIMENTAL TESTING OF AN ACCORDION
SHELL FOR AN EXPANDABLE SHELTER -
   Robert J. Morrissey

Key Words

Shelters
Response (structural)
Snow

Technical Report AMMRC TR 78-51, December 1978,
50 pp - illus-tables, D/A Project 1L162723A427
AMCMS Code 612723.4270011

The Army's prototype 50-foot expandable shelter consists of a rigid shipping con-
tainer measuring about 8x20 feet x 8 feet high. The two 20-foot sides, each
comprised of four hinged, rigid panels, expand to form the floor and end walls of
an overall 20x50-foot shelter. Each expandable section is covered by an accordion-
type sandwich panel shell which serves as the roof and side walls. The goal of
this project was to evaluate the capability of the shell to sustain simulated snow
loading so that future shells could be designed more effectively. The snow load-
ing was simulated by placing plywood sheets on the shell roof incrementally.
Deflection and strain measurements were obtained at various specific locations on
the shell roof and one side wall using several telescopic measuring devices and
strain gage rosettes. These data were to be subsequently compared with an exist-
ing finite element analysis. The deflection data were basically symmetric throughout
the shell and relatively linear with the loading. The strain data were generally
linear with the loading, but fairly low in value. These relatively low strain
values were attributed to the fact that much of the structural response action of
the shell to loading took place in the shell's joints or folds.

The deflections of each of the three rows of points were symmetric about their central deflection point, i.e., points 3, 8, and 13. The deflections of these three rows of points were also relatively symmetric with one another; the central row (6-10) deflected the most, while the deflections of the other two rows were approximately equal, with row 1-5, nearest the end wall, generally deflecting slightly more than row 11-15, nearest the container.

The data plotted in Figure 27 is replotted in Figure 28, and once again the symmetry of the data is apparent. In this case the data is plotted by rows of deflection points in the Y direction rather than in the X direction (see Figures 6 and 11). Figure 28 more clearly shows the slightly greater deflection generally exhibited by points 1-5 compared to points 11-15. This effect could be related to the movement of the end wall during the testing, but that is unlikely. Referring to Table 3, all of the end wall movement occurred during or before the third loading increment was applied. The data in Figure 28 shows that it was during loading increment 4 that points 1-5 generally began to deflect significantly more than points 11-15.

Figure 29 is a sketch of how the roof deflected accumulatively in the horizontal X-Y plane after six loading increments had been applied. Notice the general symmetry of points 1-5 and 11-15. Points 1-5 all moved toward the end wall with points 1 and 2 tending to go in the -X direction, while points 4 and 5 tended to go in the X direction. Similarly, points 11-15 all moved toward the container with points 11 and 12, and 14 and 15 tending to deflect in the -X and X directions. It is interesting to note that points 11-15 deflected more than points 1-5 in the horizontal X-Y plane, whereas points 1-5 deflected more than

Figure 29. Sketch of roof deflections in the horizontal X-Y plane.
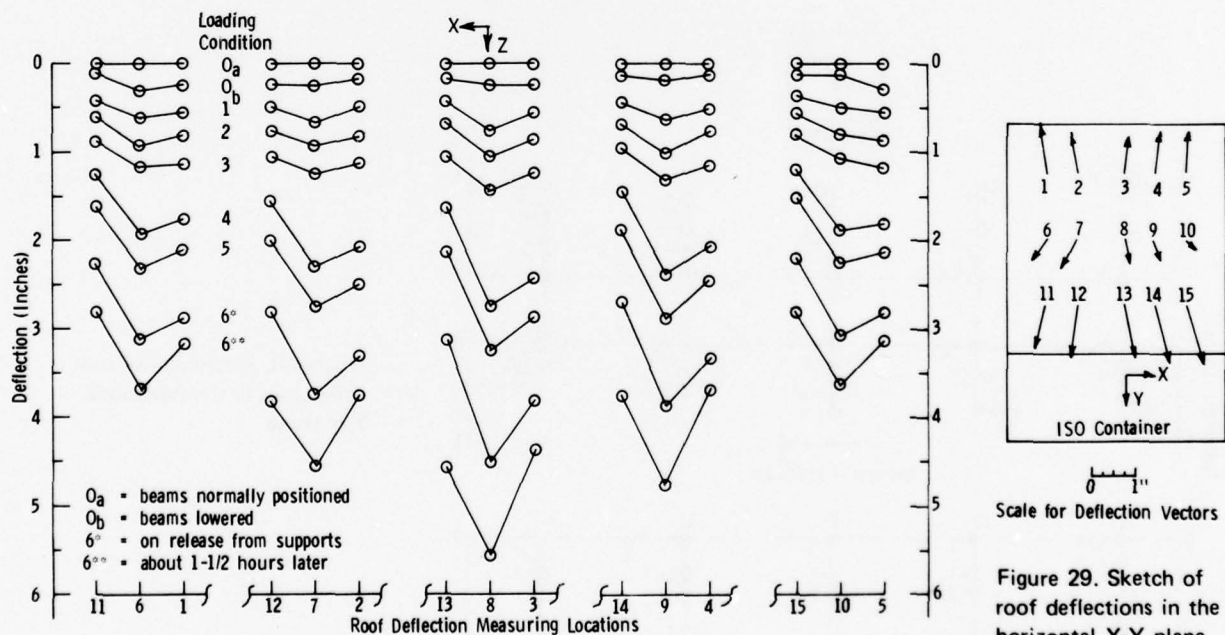
Figure 28. Accumulative roof deflections in the vertical (Z) direction plotted by rows in the Y-direction.

25

points 11-15 in the vertical Z direction (see Figures 27 and 28). Points 6-10 did not deflect as much as the other points in the horizontal plane, but these did move toward the container in a symmetric fashion similar to points 11-15.

Figure 29 was presented to aid the reader in understanding the next figure which is a plot of the roof deflection data in the horizontal X-Y plane. Figure 30 is actually 15 different plots, each traced off the graph paper on which the horizontal roof deflections were tracked with the telescopic measuring device. Any pronounced effect relating to the inward movement of the end wall during the testing should be discernible in this figure; however, such an effect is not evident here.

Figure 31 is a series of plots of accumulative roof deflections in the Y-Z plane for points 1-5, 6-10, and 11-15. These plots show how the points moved toward the container (Y direction) or end wall (-Y direction) as they deflected downward (Z direction). There does not appear to be any pronounced evidence of end wall movement and, again, there is a basic symmetry in the data.

Side Wall Deflection Measurements

The deflection measurements for the twelve side wall locations (see Figure 6) in the three directions are presented in Table 6. Figures 32, 33, and 34 are plots of these data in the X-Z, Y-Z, and X-Y planes. Figure 32 shows how the side wall points moved outward toward the vertical reference wall (X direction) as they deflected downward. Figure 33 shows how these points moved toward the container (Y direction) or end wall (-Y direction) as they deflected downward. This figure
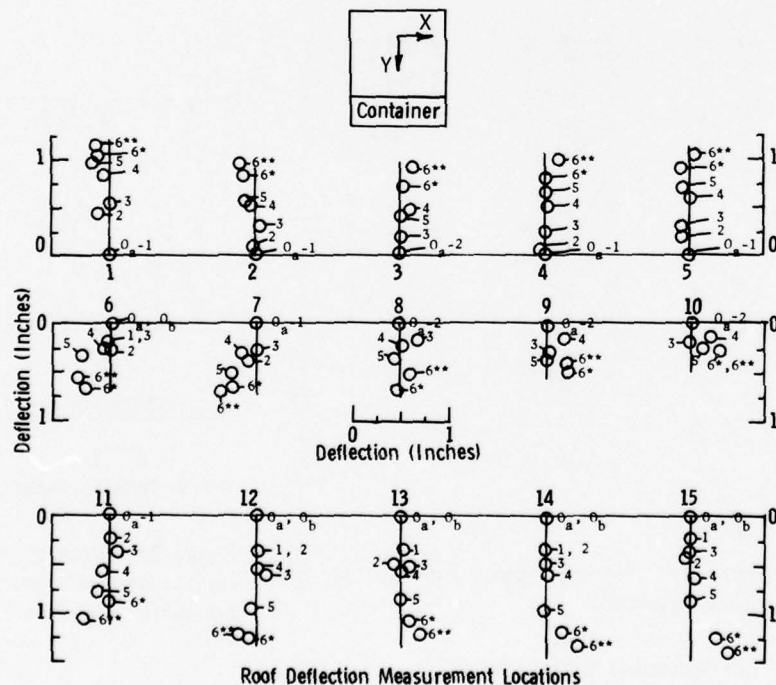
Figure 30. Accumulative roof deflections in the horizontal X-Y plane.

26
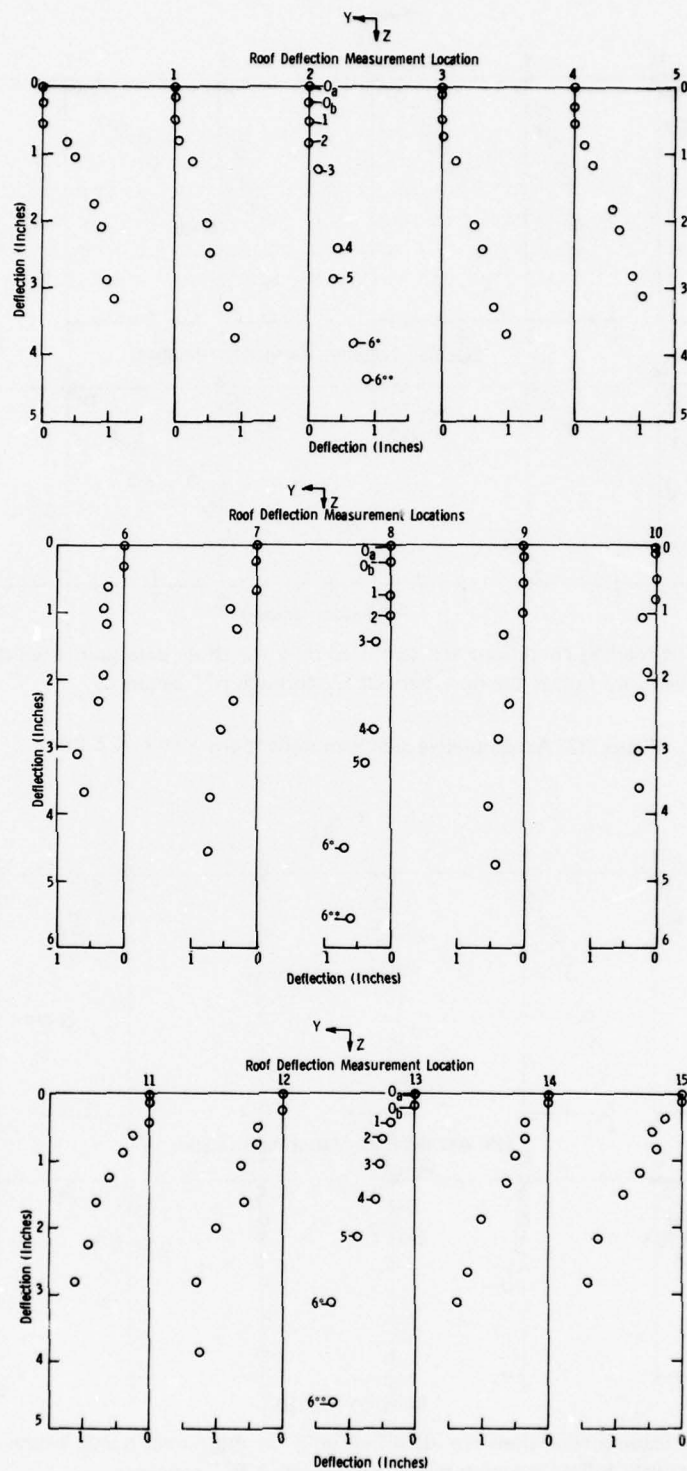
Figure 31. Accumulative roof deflections in the Y-Z plane for points 1-5, 6-10, and 11-15.
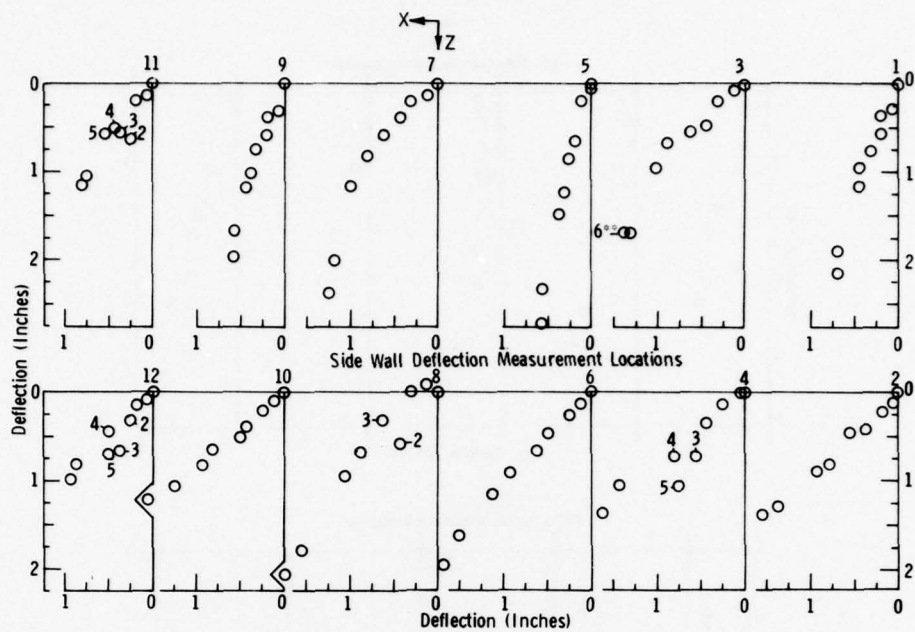
Figure 32. Accumulative side wall deflections in the X-Z plane.
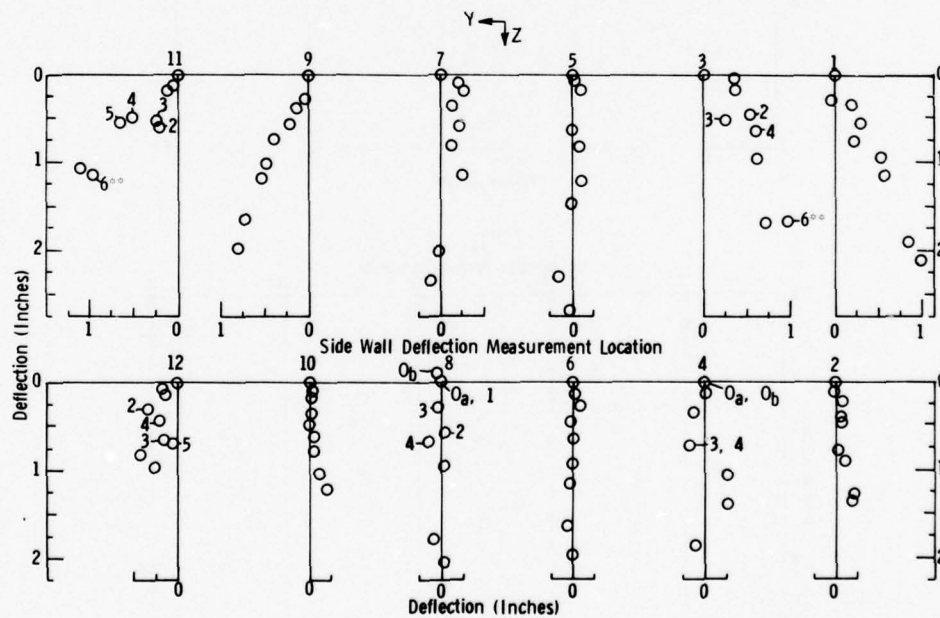
Note: The loading conditions are identified only for those data points which do not obviously follow the now familiar O_a through 6^{**} sequence.

Note: The loading conditions are identified only for those data points which do not obviously follow the now familiar O_a through 6^{**} sequence.

Figure 33. Accumulative side wall deflections in the Y-Z plane.

28

Table 6. SIDE WALL DEFLECTION MEASUREMENTS
(In Sixteenths of an Inch)
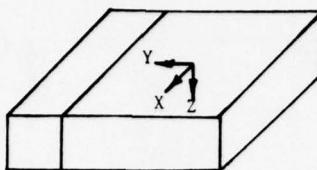
Loading Increment	X	Y	Z	X	Y	Z	X	Y	Z	X	Y	Z
	LOCATION #1			LOCATION #2			LOCATION #3			LOCATION #4		
0_a	0	0	0	0	0	0	0	0	0	0	0	0
0_b	1	1	5	1	0	2	2	-6	1	1	0	0
1	3	-3	6	3	-1	4	5	-6	3	4	0	2
2	3	-4	9	6	-1	6	7	-8	8	7	2	6
3	5	-3	12	9	-1	7	10	-4	9	9	3	12
4	7	-8	15	13	-1	13	14	-9	10	13	3	12
5	7	-9	19	15	-2	14	16	-10	15	12	-4	17
6*	11	-13	30	22	-3	20	21	-15	27	23	-4	22
6**	11	-16	34	25	-3	22	22	-11	27	26	2	30
	LOCATION #5			LOCATION #6			LOCATION #7			LOCATION #8		
0_a	0	0	0	0	0	0	0	0	0	0	0	0
0_b	0	0	1	2	0	2	2	-3	2	2	1	-1
1	2	-1	3	4	-1	4	5	-4	3	5	0	0
2	3	0	11	8	0	7	7	-2	6	7	1	9
3	4	-1	13	10	0	11	10	-3	10	10	-1	5
4	5	-1	20	15	0	15	13	-2	13	14	2	11
5	6	0	24	18	1	19	16	-4	19	17	0	15
6*	9	3	37	24	1	26	19	0	32	25	2	28
6**	9	1	43	27	0	31	20	2	38	28	-1	33
	LOCATION #9			LOCATION #10			LOCATION #11			LOCATION #12		
0_a	0	0	0	0	0	0	0	0	0	0	0	0
0_b	1	1	5	2	0	2	1	1	2	1	3	1
1	3	2	6	4	0	3	3	2	3	3	2	2
2	3	4	9	7	0	6	4	3	10	4	6	5
3	5	6	12	8	0	8	6	4	9	6	3	11
4	6	8	16	13	-1	10	7	8	8	8	4	9
5	7	9	19	15	-1	13	9	11	9	8	1	11
6*	9	12	27	20	-2	17	12	18	17	14	7	13
6**	9	13	32	25	-3	19	13	16	18	15	4	16

*Deflection measurements taken after freed from overnight settlement.
**Deflection measurements taken 1-1/2 hours later.

is actually 12 different plots, each traced off the graph papers on which these deflections were tracked using the telescopic measuring devices. Figure 34 shows similar plots for the deflections in the horizontal X-Y plane. The data presented in these three figures reveal a general symmetry of the deflection data about the center of the side wall.

Strain Measurements

Strain measurements were obtained using 42 channels of data for 30 different loading conditions (including balance and creep checks, etc.), or over 1200 "bits" of data. Although these data are the actual strain history of the gages, they contain various changes in strain values which are largely associated with balance or creep checks and therefore not directly related to the loading/unloading of the shell. Figure 35, for example, is a plot of the actual strain data from rosette
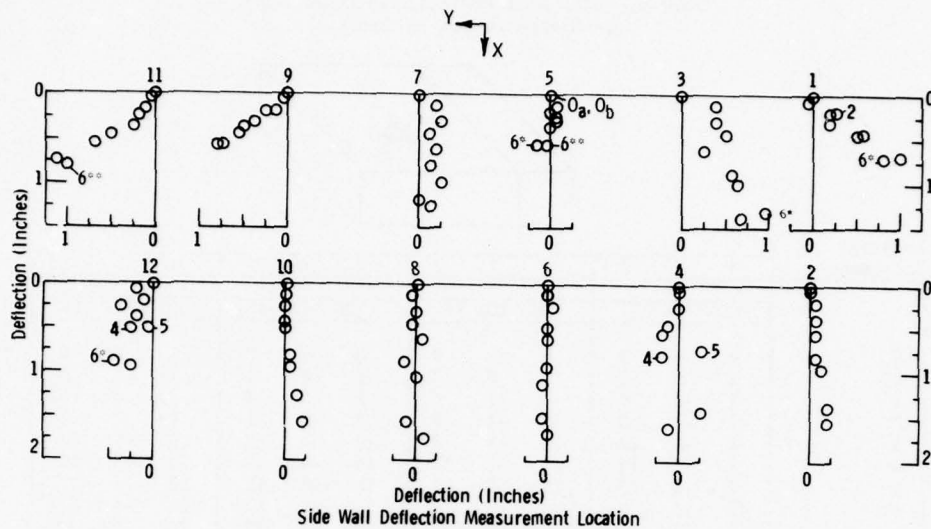
Note: The loading conditions are identified only for those data points which do not obviously follow the now familiar O_a through 6^{**} sequence.

Figure 34. Accumulative side wall deflections in the X-Y plane.
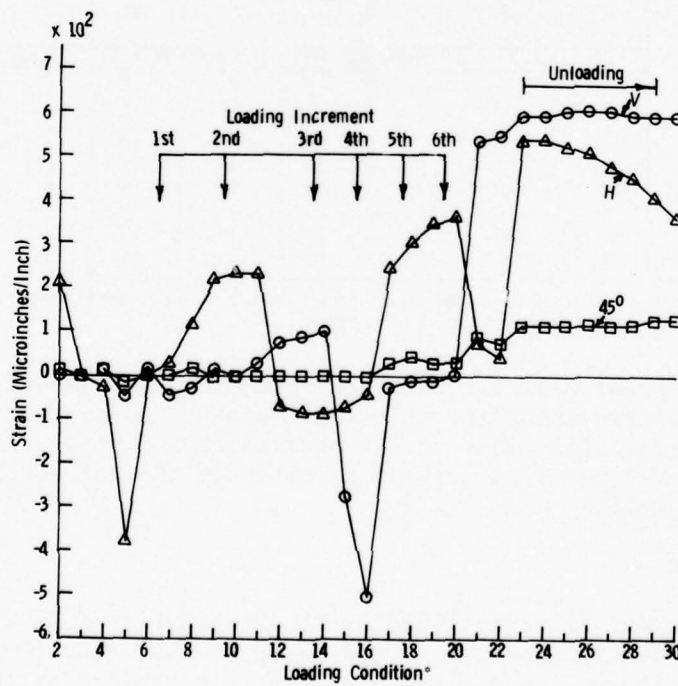
Figure 35. Accumulative strain measurements for Rosette 7_i.

*These are identified in Appendix B

7_i. This figure shows some sudden shifts in strain values and, because of these shifts, the strain values measured after unloading did not approach the values recorded just prior to applying the first loading increment.

If strain measurements made for various checks are eliminated from the data, and only the accumulative delta strains resulting from loading and unloading the shell are taken into account, the resulting data are as shown in Tables 7 and 8 and as plotted in Figure 36. The data still reveal some sudden shifts in strain values, but the curves are generally smooth and the strain values upon unloading generally approach the initial strain values taken prior to loading. The strain data from rosette 7_i is plotted in Figure 36n and may be compared with Figure 35.

The data in the strain tables are for rosettes 1_o and 1_i through 7_o and 7_i in the vertical (V), 45°, and horizontal (H) directions. Figures 6 and 8 identify the location of these rosettes on the accordion shell and also identify what is meant by V, 45°, and H. For example, V might mean straight up the slope of a roof panel, rather than vertical with respect to the earth. The strain tables in Appendix B identify each loading condition and give the date and time of each strain reading (i.e., millivolt readings which were subsequently converted to strain readings). Incidentally, the smallest reading which could be read on the data logger was 0.01 millivolt. This corresponds to slightly more than 14 microinches/inch of strain and accounts for the strain varying by increments of this amount in the data.

Table 7. ACCUMULATIVE STRAINS DURING LOADING/UNLOADING FOR ROSETTES 1-4
(Microinches per Inch)

		V	45°	H	V	45°	H	V	45°	H	V	45°	H
		ROSETTE 1_o			ROSETTE 1_i			ROSETTE 2_o			ROSETTE 2_i		
LOADING	0	0	0	0	0	0	0	0	0	0	0	0	0
	1	-14	29	-145	14	-202	-58	-29	29	116	15	58	29
	2	-28	72	-246	14	-216	-87	-29	73	116	30	89	57
	3	-41	113	-376	28	-201	-101	-43	117	131	59	147	114
	4	-41	128	-506	57	-187	-130	-130	435	203	102	493	373
	5	-26	157	-636	86	-173	-145	-130	478	-893	115	565	460
	6	-40	200	-866	114	-187	-174	-173	594	-850	131	724	691
UNLOADING	6	-56	200	-909	128	-187	-188	-188	565	-864	144	724	706
	5	-56	200	-894	114	-187	-188	-188	565	-850	131	710	662
	4	-40	156	-707	85	-187	-145	-173	522	-850	131	623	533
	3	-25	142	-577	56	-173	-101	-144	479	-879	117	522	403
	2	3	98	-433	27	-187	-73	-130	421	-908	103	407	259
	1	18	70	-188	-59	-230	-1	-73	349	-908	59	191	28
		ROSETTE 3_o			ROSETTE 3_i			ROSETTE 4_o			ROSETTE 4_i		
LOADING	0	0	0	0	0	0	0	0	0	0	0	0	0
	1	-14	-43	14	-29	-29	-14	29	29	101	-15	0	14
	2	-14	-58	28	-44	-58	-14	43	43	173	-15	15	28
	3	-29	-101	28	-58	-87	-29	43	57	244	-15	15	42
	4	-29	-145	42	-87	-102	-43	57	71	317	-44	15	57
	5	-29	-173	56	-87	-102	-43	57	84	389	-44	29	70
	6	-29	-204	71	-87	-116	-58	57	71	476	-44	42	101
UNLOADING	6	-43	-218	42	-101	-129	-72	26	56	418	-44	28	86
	5	-29	-204	42	-87	-129	-72	26	56	375	-30	28	86
	4	-29	-175	28	-87	-100	-58	26	42	303	-30	13	57
	3	-14	-146	28	-72	-85	-43	13	42	216	-16	-16	29
	2	-29	-131	-1	-87	-71	-43	-1	13	115	-1	-30	29
	1	-14	-59	-15	-72	-28	-29	-1	-2	58	28	-3	0

LOADING/UNLOADING INCREMENTS

31
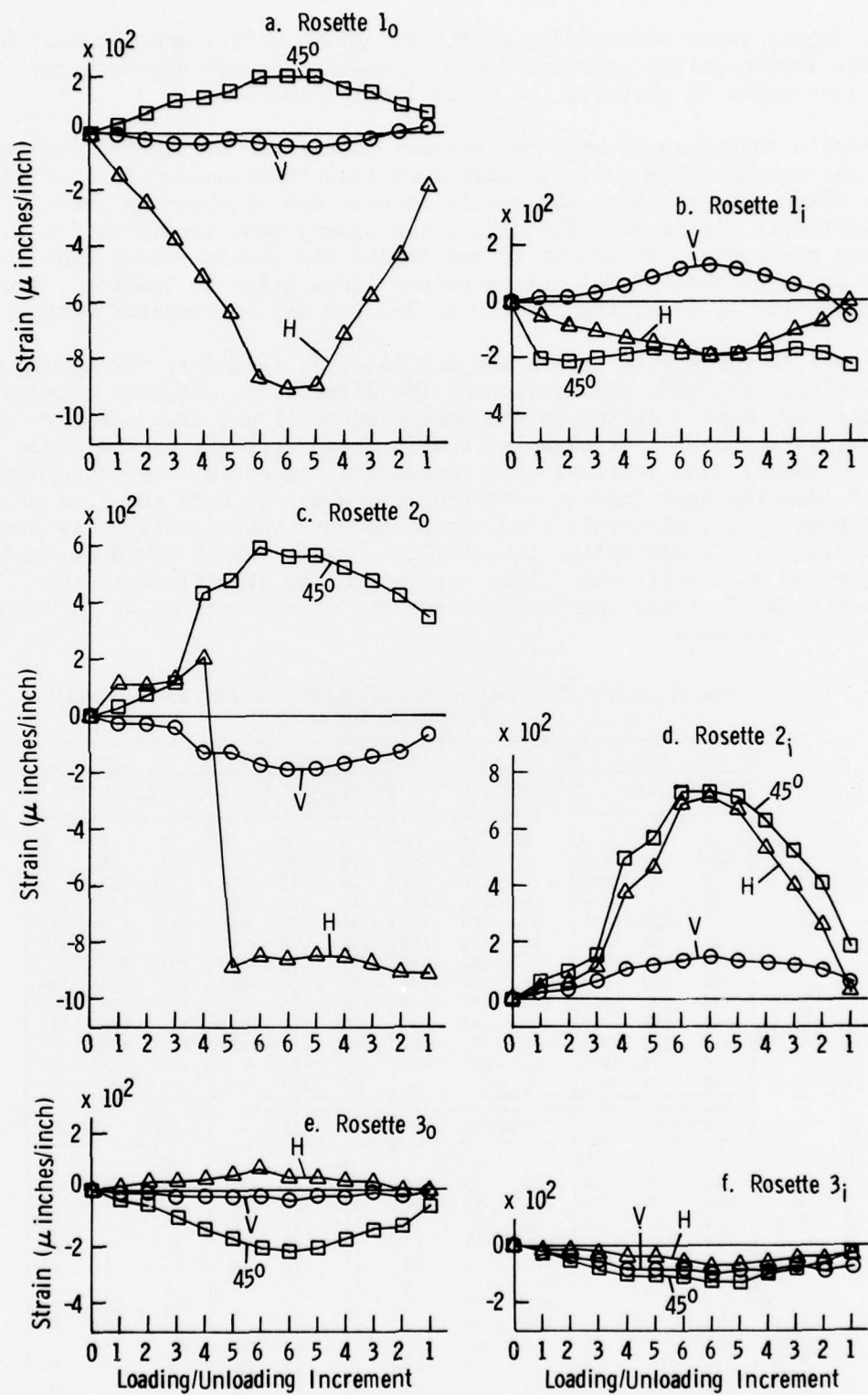
Figure 36a-f. Accumulative strains during loading/unloading.
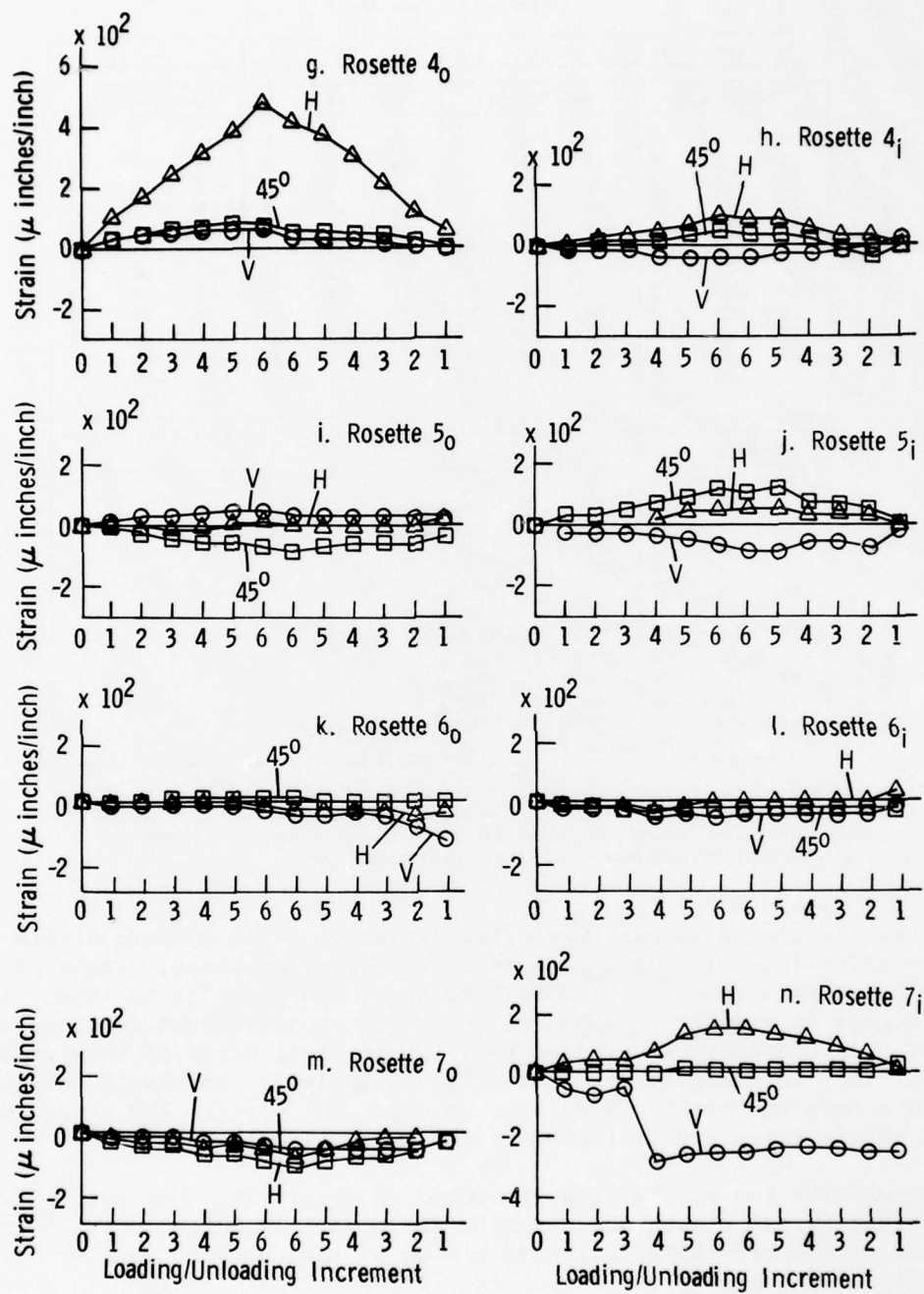
Figure 36g-n. Accumulative strains during loading/unloading.

Table 8. ACCUMULATIVE STRAINS DURING LOADING/UNLOADING FOR ROSETTES 5-7
(Microinches per Inch)

		V	45°	H	V	45°	H	V	45°	H	V	45°	H
		ROSETTE 5_o			ROSETTE 5_i			ROSETTE 6_o			ROSETTE 6_i		
LOADING	0	0	0	0	0	0	0*	0	0	0	0	0	0
	1	14	-15	0	-28	29		-14	0	0	-28	-14	-14
	2	28	-30	-15	-28	29		-14	0	0	-28	-14	-14
	3	28	-44	-15	-28	43		-14	15	0	-28	-29	-14
	4	42	-58	0	-42	72	14	-14	15	0	-57	-44	-28
	5	42	-58	14	-57	87	42	-14	15	0	-43	-30	-14
	6	42	-73	14	-72	116	42	-27	15	-14	-57	-30	1
UNLOADING	6	28	-87	0	-86	102	55	-56	15	-29	-43	-30	1
	5	28	-73	0	-86	116	55	-56	-1	-29	-43	-30	1
	4	28	-60	0	-57	73	28	-42	-1	-29	-43	-30	1
	3	28	-60	0	-57	73	28	-56	-1	-29	-43	-30	1
	2	28	-60	0	-72	58	28	-85	-1	-43	-43	-30	1
	1	28	-29	29	-14	15	-1	-128	-1	-29	-14	-30	30

		V	45°	H	V	45°	H
		ROSETTE 7_o			ROSETTE 7_i		
LOADING	0	0	0	0	0	0	0
	1	-14	-28	-14	-57	0	29
	2	-14	-42	-28	-71	0	44
	3	-14	-42	-28	-57	0	44
	4	-29	-71	-57	-288	0	73
	5	-29	-71	-44	-273	14	131
	6	-43	-100	-57	-259	14	145
UNLOADING	6	-57	-114	-71	-259	14	145
	5	-57	-100	-57	-244	14	130
	4	-57	-71	-28	-244	14	116
	3	-57	-71	-14	-244	14	87
	2	-57	-57	-14	-259	14	58
	1	-30	-28	†	-259	27	15

(Left vertical label: LOADING/UNLOADING INCREMENTS)

*The terminal wires to this gage (5_iH) were resoldered just prior to applying the
forth loading increment; data obtained earlier from this gage are not valid.
†For some unexplained reason, the print-out from the data logger omitted a
reading necessary to determine the strain measurement here.

Prior to testing, a strain gage within rosette 1_i and another within 4_i were
found to be defective. To obtain readings for these locations, single gages were
mounted in close proximity to the defective gages and parallel to them. In addi-
tion, the H gage of rosette 5_i appeared to be giving irrelevant readings during
the testing. An examination revealed that the terminal wires of this gage had
come loose. They were resoldered just prior to applying the fourth loading in-
crement; data obtained earlier from this gage are not valid. The irregularities
found with strain gages are footnoted in the appropriate tables.

Let us examine the strain data presented in Figure 36. One observation is
that the values of the strain measurements are generally quite low. The reason
is that much of the structural response action of the shell to loading occurred
in the joints of the shell, and during the latter part of testing, in creating
failure characteristics as well. It is also noted that the strain values from
rosettes 1-4 were generally higher for the gages applied to the outside of the
shell, compared to those applied inside. Again, this is probably related to the
structural response nature of the shell, whereby the inner face-sheets were
stressed to a relatively low level because much of the action was taking place

34

at the joints. Another observation is that the largest strains were detected by rosettes 1_o, 1_i, 2_o, and 2_i. These rosettes were located close to the symmetric fabrication joint (see Figure 6), which was misaligned by shearing action during the testing.

Because of their similar locations and orientations (see Figures 6 and 8), one would expect that the strain data from rosettes 1_o and 3_o would be similar and also that the data from rosettes 2_o and 4_o would be similar. The data from rosettes 1_o and 3_o are plotted in Figures 36a and e. The largest tensile strain for rosette 1_o was recorded by the 45° gage, whereas for rosette 3_o it was recorded by the H gage. Similarly, the largest compressive strain was recorded by the H gage for rosette 1_o and by the 45° gage for rosette 3_o. The data from rosettes 2_o and 4_o are plotted in Figure 36c and g. Although the H gage of rosette 2_o recorded a sudden unexplainable shift, we can still compare the data. The largest tensile strain for rosette 2_o was recorded by the 45° gage, whereas for rosette 4_o it was recorded by the H gage. The V gage for rosette 2_o recorded compressive strains throughout the loading and unloading, whereas the V gage of rosette 4_o recorded tensile strains. Hence, the data is not as similar as one would expect.

Rosettes 7_o and 7_i were located fairly close to an interbay column base which was crushed during the testing (Figure 21a). The data from rosettes 7_o and 7_i are plotted in Figures 36m and n. The V gage of rosette 7_i recorded a sizable increase in compressive strain as the fourth loading increment was applied. Since we first noticed that some of the interbay column bases were crushing just after that increment was applied, this strain increase could be related to the base crushing action. However, we did not take note as to whether or not this particular base began crushing at that time.

Additionally, NARADCOM personnel made a preliminary comparison between this strain data and the finite element analysis. This comparison revealed a general agreement in terms of regions of high or low tensile or compressive strains.

DISCUSSION

The original objectives of this investigation were to obtain deflection and strain data at specific locations on the accordion shell as the shell roof was loaded incrementaly to about ten pounds per square foot over the projected area. The 10-pound goal was not reached because of the imminent collapse of the shell after about 4-1/2 pounds had been applied.

Another objective was to conduct this investigation efficiently in terms of obtaining the results fairly quickly and inexpensively. The shelter was transported to AMMRC in mid-March 1978. After 2-1/2 months of preparation the testing was performed as six increments of loading were applied to the shell roof in 1-1/2 days of testing. The data obtained included over 700 deflection measurements and over 1200 strain measurements. These data were all reduced (i.e., converted, tabulated, and plotted) and supplied to NARADCOM within a month, with this report to follow.

The deflection data was generally symmetric about the accordion shell roof and side wall. The values of the strain data were generally relatively low. The basic reason for this is because much of the structural response action of the shell to loading took place in the joints of the shell. Nevertheless, a preliminary comparison of the strain data with the finite element analysis by NARADCOM personnel revealed general agreement in terms of regions of high or low tensile or compressive strains.

The telescopic measuring devices, designed during this investigation to be used in conjunction with a scale and reference planes, proved to be an efficient way to obtain three-dimensional deflection measurements. The manner in which two thicknesses of plywood sheets were positioned on the shell roof to simulate snow loading resulted in a fairly uniformly distributed load over the projected area.

In summary, the objectives of this investigation were met except that the loading had to be terminated before anticipated to prevent significant damage to the accordion shell.

CONCLUSIONS

1. The deflection data obtained in this investigation appears to be quite good. The roof deflection data is fairly symmetric about both horizontal axes, with the greatest deflection occurring vertically downward at deflection point 8, the point nearest the center of the shell roof. The side wall deflection data is relatively symmetric about the center of the wide wall, with the greatest deflections generally occurring vertically downward near the middle of the side wall.

2. The relatively low values of the strain measurements are attributable to the structural response nature of the accordion shell to roof loading. Much of the response action took place in the joints of the shell and, consequently, the face-sheets to which the strain gages were applied were not stressed to a very high level.

3. The use of simply-constructed telescopic measuring devices in conjunction with a scale and reference planes proved to be an effective technique to obtain relatively accurate three-dimensional deflection measurements on structures where fairly large deflections are anticipated.

4. The way in which two thicknesses of plywood sheets were used to simulate snow loading the roof of the shell was an efficient method of achieving a fairly uniform distribution of loading over the projected area.

5. The inward movement of the end wall during the loading did not appear to have any pronounced effect in the deflection data.

6. The corrosion discovered on the inner face-sheets of the lower knees of the roof panels was apparently caused by captured rain water or melting snow eventually finding its way through cracks in joints or through punctures, and then through the core material.

RECOMMENDATIONS

The basic objective of the investigation was to obtain experimental data. We have, nevertheless, tried to make this a self-sustaining report in the sense that we have mentioned and/or referenced all of the pertinent information available to us concerning the shell's construction, its prior field testing, etc. We have also tried to provide as much detail as possible about this investigation. Following this thoroughness theme, we make the following recommendations:

1. The accordion shell was manufactured by methods which resulted in a fabrication joint running symmetrically down the middle of the shell roof, between the side walls. This joint is an obvious weak point in the shell's design. One possible solution is to modify the manufacturing machinery or methods to eliminate this joint. An alternative would be to keep this joint where it is and install a third box beam to provide support for it. There appears to be ample room in the container to transport such a beam, which would also increase the roof's snow load capacity.

2. The corrosion problem could be resolved in future shell designs by using a corrosion-resistant material for the face-sheets or, perhaps, by providing better protective coatings, etc.

3. In eracting the shelter it became obvious that the fit between the accordion shell and its attachment all around to the container, floor, and end wall was a tight one. This forced fit results in residual stresses which could reduce the structural integrity of the shell. This tightness offit aspect is also apparent in the field testing results,[4] where many of the captive fasteners were found to damage easily. In fact, recommendation number 12 from that field testing report is:

> "Redesign the expandable shells for easier interface with the
>   container, and walls, and floor."[4]

We concur with that recommendation and also suggest that more effective captive fasteners be used on shells designed in the future.

ACKNOWLEDGMENTS

APPENDIX A. PRELIMINARY TEST ON SECTION OF SHELL ROOF

It was noted that actual snow loading would initially concentrate in the valleys between the roof ridges, whereas the simulated snow loading with plywood sheets would concentrate the loading on the ridges. NARADCOM had provided a section of a shell roof bay which was tested for localized crippling under loading at the shell ridge. We also measured strains from rosettes identical to those to be used on the actual shell. The results of this test are shown in Figure A-1 along with a sketch of the test setup and strain directions. The test jig consisted of a plywood sheet with two pieces of 2x4's nailed to it parallel to each other about 36 inches apart. Another piece of 2x4 (representing a two-pound preload) was placed symmetrically on the ridge. The section was loaded by placing dead weights on top of this piece of 2x4 in 10-pound increments to 62 pounds (or almost 14 pounds per square foot over the projected area), then unloaded with no visible localized crippling effects. The measured strain values were quite small. It was noted that the lower "knees" were supported in this test, whereas they would not be supported in testing the accordion shell except where they intersected the side walls.
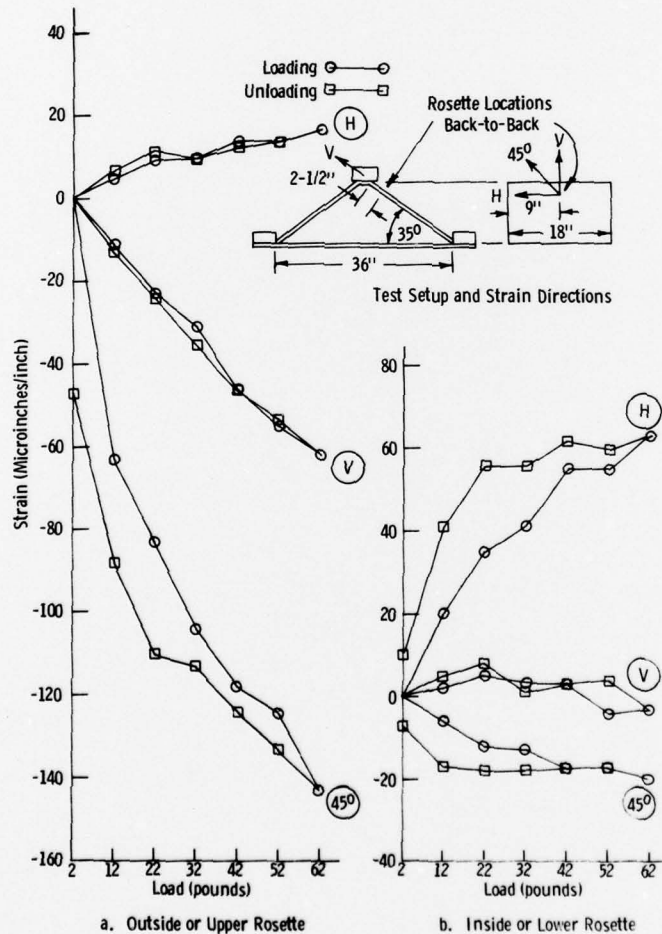
Figure A-1. Preliminary test on section of shell roof.

APPENDIX B. ACCUMULATIVE STRAIN DATA

The accumulative strain data for rosettes 1_o and 1_i through 7_o and 7_i are presented in Tables B-1 through B-7. Each loading condition is identified in these tables and the time and date of each strain reading is also shown.

Table B-1. ACCUMULATIVE STRAINS FOR ROSETTES 1_o AND 1_i (Microinches/inch)

No.	LOADING CONDITION	DATE (1978)	TIME	ROSETTE 1_o			ROSETTE 1_i		
				V	45°	H	V*	45°	H
1	0_a No Load, Beams Normal	6 June	2:15 p.m.	0	0	0	0	0	0
2	0_b No Load, Beams Lowered	"	3:15 p.m.	115	43	-58	144	128	14
3	Null Balance	"	3:40 p.m.	0	0	0	0	0	0
4	Balance Check	"	4:30 p.m.	43	0	0	-14	0	0
5	Overnight Balance Check	7 June	8:00 a.m.	-159	-72	-58	-14	-72	-43
6	Before 1st Loading Increment	"	1:30 p.m.	0	14	-14	0	29	0
7	After 1st Loading Increment	"	2:10 p.m.	-14	43	-159	14	-173	-58
8	Creep Check	"	2:30 p.m.	29	43	-144	43	-159	-29
9	Before 2nd Loading Increment	"	3:35 p.m.	101	58	0	0	-159	-29
10	After 2nd Loading Increment	"	3:50 p.m.	87	101	-101	0	-173	-58
11	Creep Check	"	4:15 p.m.	87	87	-101	0	-173	-58
12	Overnight Creep Check	8 June	8:30 a.m.	-101	87	-14	29	-187	-58
13	Before 3rd Loading Increment	"	9:40 a.m.	-115	87	-14	29	-202	-58
14	After 3rd Loading Increment	"	10:05 a.m.	-128	128	-144	43	-187	-72
15	Before 4th Loading Increment	"	11:50 a.m.	-115	144	-144	43	-187	-72
16	After 4th Loading Increment	"	11:55 a.m.	-115	159	-274	72	-173	-101
17	Before 5th Loading Increment	"	2:50 p.m.	72	274	-274	115	-101	-14
18	After 5th Loading Increment	"	2:58 p.m.	87	303	-404	144	-87	-29
19	Before 6th Loading Increment	"	3:45 p.m.	101	317	-433	159	-101	-43
20	After 6th Loading Increment	"	3:55 p.m.	87	360	-663	187	-115	-72
21	Settled on Supports Overnight	9 June	8:30 a.m.	-14	360	-461	128	-115	87
22	On Removal of Supports	"	9:30 a.m.	-43	404	-620	173	-115	58
23	Before Unloading 6th Increment	"	2:30 p.m.	144	433	-433	260	29	187
24	Before Unloading 5th Increment	"	2:35 p.m.	128	433	-476	274	29	173
25	Before Unloading 4th Increment	"	2:40 p.m.	128	433	-461	260	29	173
26	Before Unloading 3rd Increment	"	2:43 p.m.	144	389	-274	231	29	216
27	Before Unloading 2nd Increment	"	2:46 p.m.	159	375	-144	202	43	260
28	Before Unloading 1st Increment	"	2:49 p.m.	187	331	0	173	29	288
29	Fully Unloaded	"	2:53 p.m.	202	303	245	87	-14	360
30	Permanent Set Check	"	3:21 p.m.	187	288	216	87	0	375

* This gage was found to be defective so these readings were obtained from a single strain gage mounted parallel to gage 1_iV, but about one half inch lower than 1_iV.

41

Table B-2. ACCUMULATIVE STRAINS FOR ROSETTES 2_o AND 2_i (Microinches/inch)

No.	LOADING CONDITION	DATE (1978)	TIME	ROSETTE 2_o 45°			ROSETTE 2_i 45°		
				V	45°	H	V	45°	H
1	0 No Load, Beams Normal	6 June	2:15 p.m.	0	0	0	0	0	0
2	0^a No Load, Beams Lowered	"	3:15 p.m.	-14	72	87	29	43	159
3	Null Balance	"	3:40 p.m.	0	0	0	0	0	0
4	Balance Check	"	4:30 p.m.	0	14	-101	0	0	29
5	Overnight Balance Check	7 June	8:00 a.m.	-58	43	187	-29	-101	-14
6	Before 1st Loading Increment	"	1:30 p.m.	-14	0	43	14	14	14
7	After 1st Loading Increment	"	2:10 p.m.	-43	29	159	29	72	43
8	Creep Check	"	2:30 p.m.	-29	72	836	43	87	58
9	Before 2nd Loading Increment	"	3:35 p.m.	-43	115	43	43	128	87
10	After 2nd Loading Increment	"	3:50 p.m.	-43	159	43	58	159	115
11	Creep Check	"	4:15 p.m.	-58	159	58	72	159	115
12	Overnight Creep Check	8 June	8:30 a.m.	0	0	707	58	29	0
13	Before 3rd Loading Increment	"	9:40 a.m.	-14	14	735	58	14	-14
14	After 3rd Loading Increment	"	10:05 a.m.	-14	58	750	87	72	43
15	Before 4th Loading Increment	"	11:50 a.m.	29	115	-173	58	87	58
16	After 4th Loading Increment	"	11:55 a.m.	-58	433	-101	101	433	317
17	Before 5th Loading Increment	"	2:50 p.m.	29	606	1240	115	505	418
18	After 5th Loading Increment	"	2:58 p.m.	29	649	144	128	577	505
19	Before 6th Loading Increment	"	3:45 p.m.	43	692	245	128	591	548
20	After 6th Loading Increment	"	3:55 p.m.	0	808	288	144	750	779
21	Settled on Supports Overnight	9 June	8:30 a.m.	216	1154	1168	115	750	663
22	On Removal of Supports	"	9:30 a.m.	173	1312	1255	159	880	937
23	Before Unloading 6th Increment	"	2:30 p.m.	231	1658	1615	115	1067	1211
24	Before Unloading 5th Increment	"	2:35 p.m.	216	1629	1601	128	1067	1226
25	Before Unloading 4th Increment	"	2:40 p.m.	216	1629	1615	115	1053	1182
26	Before Unloading 3rd Increment	"	2:43 p.m.	231	**1586**	1615	115	966	1053
27	Before Unloading 2nd Increment	"	2:46 p.m.	260	1543	1586	101	865	923
28	Before Unloading 1st Increment	"	2:49 p.m.	274	1485	1557	87	750	779
29	Fully Unloaded	"	2:53 p.m.	331	1413	1557	43	534	548
30	Permanent Set Check	"	3:21 p.m.	375	1341	1543	72	346	360

42

Table B-3. ACCUMULATIVE STRAINS FOR ROSETTES 3_o AND 3_i (Microinches/inch)

No.	LOADING CONDITION	DATE (1978)	TIME	ROSETTE 3_o V	45°	H	ROSETTE 3_i V	45°	H
1	0 No Load, Beams Normal	6 June	2:15 p.m.	0	0	0	0	0	0
2	0[a] No Load, Beams Lowered	"	3:15 p.m.	29	14	14	0	0	14
3	0[b] Null Balance	"	3:40 p.m.	0	0	0	0	0	0
4	Balance Check	"	4:30 p.m.	0	0	0	0	0	29
5	Overnight Balance Check	7 June	8:00 a.m.	-173	-87	-14	-43	-14	-43
6	Before 1st Loading Increment	"	1:30 p.m.	0	14	87	-14	-29	0
7	After 1st Loading Increment	"	2:10 p.m.	-14	-29	101	-43	-14	-14
8	Creep Check	"	2:30 p.m.	0	-14	101	-43	-43	0
9	Before 2nd Loading Increment	"	3:35 p.m.	0	-14	101	-43	-29	0
10	After 2nd Loading Increment	"	3:50 p.m.	0	-29	115	-58	-58	0
11	Creep Check	"	4:15 p.m.	0	-43	101	-43	-43	0
12	Overnight Creep Check	8 June	8:30 a.m.	-14	-101	159	-58	-43	-43
13	Before 3rd Loading Increment	"	9:40 a.m.	-14	-101	173	-58	-43	-43
14	After 3rd Loading Increment	"	10:05 a.m.	-29	-144	173	-72	-72	-58
15	Before 4th Loading Increment	"	11:50 a.m.	0	-115	202	-43	29	-29
16	After 4th Loading Increment	"	11:55 a.m.	0	-159	216	-72	14	-43
17	Before 5th Loading Increment	"	2:50 p.m.	87	-87	274	-14	14	58
18	After 5th Loading Increment	"	2:58 p.m.	87	-115	288	-14	14	58
19	Before 6th Loading Increment	"	3:45 p.m.	87	-128	288	-29	14	58
20	After 6th Loading Increment	"	3:55 p.m.	87	-159	303	-29	0	43
21	Settled on Supports Overnight	9 June	8:30 a.m.	173	-128	346	-14	29	115
22	On Removal of Supports	"	9:30 a.m.	173	-173	360	-14	173	128
23	Before Unloading 6th Increment	"	2:35 p.m.	245	-87	389	43	128	245
24	Before Unloading 5th Increment	"	2:40 p.m.	231	-101	360	29	115	231
25	Before Unloading 4th Increment	"	2:43 p.m.	245	-87	360	43	115	231
26	Before Unloading 3rd Increment	"	2:46 p.m.	245	-58	346	43	144	245
27	Before Unloading 2nd Increment	"	2:49 p.m.	260	-29	346	58	159	260
28	Before Unloading 1st Increment	"	2:53 p.m.	245	-14	317	43	173	260
29	Fully Unloaded	"	3:21 p.m.	260	58	303	58	216	274
30	Permanent Set Check	"	3:21 p.m.	260	43	288	58	202	274

Table B-4. ACCUMULATIVE STRAINS FOR ROSETTES 4_o AND 4_i (Microinches/inch)

No.	LOADING CONDITION	DATE (1978)	TIME	ROSETTE 4_o V	45°	H	ROSETTE 4_i V	45°	H*
1	O No Load, Beams Normal	6 June	2:15 p.m.	0	0	0	0	0	0
2	O_a No Load, Beams Lowered	"	3:15 p.m.	0	-14	29	14	43	43
3	Null Balance	"	3:40 p.m.	0	0	0	0	0	0
4	Balance Check	"	4:30 p.m.	-29	0	-14	0	0	0
5	Overnight Balance Check	7 June	8:00 a.m.	-29	0	14	-14	-87	-14
6	Before 1st Loading Increment	"	1:30 p.m.	14	0	43	58	-14	0
7	After 1st Loading Increment	"	2:10 p.m.	43	29	144	43	-14	14
8	Creep Check	"	2:30 p.m.	29	14	144	58	0	29
9	Before 2nd Loading Increment	"	3:35 p.m.	29	29	144	58	14	29
10	After 2nd Loading Increment	"	3:50 p.m.	43	43	216	58	29	43
11	Creep Check	"	4:15 p.m.	43	43	216	58	14	43
12	Overnight Creep Check	8 June	8:30 a.m.	72	58	260	128	-29	29
13	Before 3rd Loading Increment	"	9:40 a.m.	72	58	260	144	-29	29
14	After 3rd Loading Increment	"	10:05 a.m.	72	72	331	144	-29	43
15	Before 4th Loading Increment	"	11:50 a.m.	87	87	331	202	0	72
16	After 4th Loading Increment	"	11:55 a.m.	101	101	404	173	0	87
17	Before 5th Loading Increment	"	2:50 p.m.	115	115	433	303	87	115
18	After 5th Loading Increment	"	2:58 p.m.	115	128	505	303	101	128
19	Before 6th Loading Increment	"	3:45 p.m.	128	128	519	331	115	128
20	After 6th Loading Increment	"	3:55 p.m.	128	115	606	331	128	159
21	Settled on Supports Overnight	9 June	8:30 a.m.	128	101	519	735	87	128
22	On Removal of Supports	"	9:30 a.m.	144	128	620	735	115	173
23	Before Unloading 6th Increment	"	2:30 p.m.	159	87	577	880	173	159
24	Before Unloading 5th Increment	"	2:35 p.m.	128	72	519	880	159	144
25	Before Unloading 4th Increment	"	2:40 p.m.	128	72	476	894	159	144
26	Before Unloading 3rd Increment	"	2:43 p.m.	128	58	404	894	144	115
27	Before Unloading 2nd Increment	"	2:46 p.m.	115	58	317	908	144	87
28	Before Unloading 1st Increment	"	2:49 p.m.	115	29	216	923	115	87
29	Fully Unloaded	"	2:53 p.m.	101	14	159	952	101	58
30	Permanent Set Check	"	3:21 p.m.	101	14	128	952	115	43

* This gage was found to be defective so these readings were obtained from a single strain gage mounted parallel to gage 4_iH, but about one half inch to the right of 4_iH.

Table B-5. ACCUMULATIVE STRAINS FOR ROSETTES 5_o AND 5_1 (Microinches/inch)

No.	LOADING CONDITION	DATE (1978)	TIME	ROSETTE 5_o V	45°	H	ROSETTE 5_1 V	45°	H*
1	0 No Load, Beams Normal	6 June	2:15 p.m.	0	0	0	0	0	
2	0^a No Load, Beams Lowered	"	3:15 p.m.	29	14	29	0	29	
3	Null Balance	"	3:40 p.m.	0	0	0	0	0	
4	Balance Check	"	4:30 p.m.	0	0	29	0	0	
5	Overnight Balance Check	7 June	8:00 a.m.	-72	-29	-115	-43	-29	
6	Before 1st Loading Increment	"	1:30 p.m.	0	87	29	14	29	
7	After 1st Loading Increment	"	2:10 p.m.	14	72	29	-14	58	
8	Creep Check	"	2:30 p.m.	0	58	14	-14	72	
9	Before 2nd Loading Increment	"	3:35 p.m.	29	58	87	0	87	
10	After 2nd Loading Increment	"	3:50 p.m.	43	43	72	0	87	
11	Creep Check	"	4:15 p.m.	29	29	29	0	87	
12	Overnight Creep Check	8 June	8:30 a.m.	43	14	29	-43	87	
13	Before 3rd Loading Increment	"	9:40 a.m.	72	14	29	-43	101	
14	After 3rd Loading Increment	"	10:05 a.m.	72	0	29	-43	115	
15	Before 4th Loading Increment	"	11:50 a.m.	101	14	43	-58	144	0
16	After 4th Loading Increment	"	11:55 a.m.	115	0	58	-72	173	14
17	Before 5th Loading Increment	"	2:50 p.m.	187	58	173	-43	187	-14
18	After 5th Loading Increment	"	2:58 p.m.	187	58	187	-58	202	14
19	Before 6th Loading Increment	"	3:45 p.m.	202	58	202	-43	202	14
20	After 6th Loading Increment	"	3:55 p.m.	202	43	202	-58	231	14
21	Settled on Supports Overnight	9 June	8:30 a.m.	288	72	187	-14	245	72
22	On Removal of Supports	"	9:30 a.m.	303	72	187	-14	288	87
23	Before Unloading 6th Increment	"	2:30 p.m.	360	115	288	14	274	115
24	Before Unloading 5th Increment	"	2:35 p.m.	346	101	274	0	260	128
25	Before Unloading 4th Increment	"	2:40 p.m.	346	115	274	0	274	128
26	Before Unloading 3rd Increment	"	2:43 p.m.	346	128	274	29	231	101
27	Before Unloading 2nd Increment	"	2:46 p.m.	346	128	274	29	231	101
28	Before Unloading 1st Increment	"	2:49 p.m.	346	128	274	14	216	101
29	Fully Unloaded	"	2:53 p.m.	346	159	303	72	173	72
30	Permanent Set Check	"	3:21 p.m.	331	144	303	72	173	72

* The terminal wires to this gage were resoldered just prior to applying the 4th loading increment; data obtained earlier from this gage are not valid.

Table B-6. ACCUMULATIVE STRAINS FOR ROSETTES 6_o AND 6_i (Microinches/inch)

No.	LOADING CONDITION	DATE (1978)	TIME	ROSETTE 6_o			ROSETTE 6_i		
				V	45°	H	V	45°	H
1	No Load, Beams Normal	6 June	2:15 p.m.	0	0	0	0	0	0
2	0^a No Load, Beams Lowered	"	3:15 p.m.	14	0	29	0	29	0
3	Null Balance	"	3:40 p.m.	0	0	0	0	0	0
4	Balance Check	"	4:30 p.m.	0	14	14	0	-14	14
5	Overnight Balance Check	7 June	8:00 a.m.	0	-43	-87	-58	-87	14
6	Before 1st Loading Increment	"	1:30 p.m.	14	14	14	14	0	0
7	After 1st Loading Increment	"	2:10 p.m.	0	14	14	-14	-14	-14
8	Creep Check	"	2:30 p.m.	0	29	29	0	0	0
9	Before 2nd Loading Increment	"	3:35 p.m.	43	29	29	0	0	0
10	After 2nd Loading Increment	"	3:50 p.m.	43	29	29	0	0	0
11	Creep Check	"	4:15 p.m.	0	29	14	0	0	0
12	Overnight Creep Check	8 June	8:30 a.m.	43	29	-29	-14	-29	0
13	Before 3rd Loading Increment	"	9:40 a.m.	43	14	-29	-14	-43	0
14	After 3rd Loading Increment	"	10:05 a.m.	43	29	-29	-14	-58	0
15	Before 4th Loading Increment	"	11:50 a.m.	115	29	-29	0	-43	14
16	After 4th Loading Increment	"	11:55 a.m.	115	29	-29	-29	-58	0
17	Before 5th Loading Increment	"	2:50 p.m.	216	87	58	29	0	29
18	After 5th Loading Increment	"	2:58 p.m.	216	87	58	43	14	43
19	Before 6th Loading Increment	"	3:45 p.m.	128	87	72	43	14	14
20	After 6th Loading Increment	"	3:55 p.m.	115	87	58	29	14	29
21	Settled on Supports Overnight	9 June	8:30 a.m.	187	101	29	115	0	58
22	On Removal of Supports	"	9:30 a.m.	216	87	29	115	14	43
23	Before Unloading 6th Increment	"	2:30 p.m.	476	144	87	159	43	72
24	Before Unloading 5th Increment	"	2:35 p.m.	447	144	72	173	43	72
25	Before Unloading 4th Increment	"	2:40 p.m.	447	128	72	173	43	72
26	Before Unloading 3rd Increment	"	2:43 p.m.	461	128	72	173	43	72
27	Before Unloading 2nd Increment	"	2:46 p.m.	447	128	72	173	43	72
28	Before Unloading 1st Increment	"	2:49 p.m.	418	128	58	173	43	72
29	Fully Unloaded	"	2:53 p.m.	375	128	72	202	43	101
30	Permanent Set Check	"	3:21 p.m.	375	115	58	202	43	101

46

Table B-7. ACCUMULATIVE STRAINS FOR ROSETTES γ_o AND γ_i (Microinches/inch)

No.	LOADING CONDITION	DATE (1978)	TIME	ROSETTE γ_o V	45°	H	ROSETTE γ_i V	45°	H
1	O No Load, Beams Normal	6 June	2:15 p.m.	0	0	0	0	0	0
2	O^a No Load, Beams Lowered	"	3:15 p.m.	14	0	-14	0	14	216
3	Null Balance	"	3:40 p.m.	0	0	0	0	0	0
4	Balance Check	"	4:30 p.m.	0	0	14	14	14	-29
5	Overnight Balance Check	7 June	8:00 a.m.	-29	-58	14	-43	-14	-375
6	Before 1st Loading Increment	"	1:30 p.m.	14	14	101	14	0	0
7	After 1st Loading Increment	"	2:10 p.m.	0	-14	87	-43	0	29
8	Creep Check	"	2:30 p.m.	14	0	87	-29	14	115
9	Before 2nd Loading Increment	"	3:35 p.m.	0	0	101	14	0	216
10	After 2nd Loading Increment	"	3:50 p.m.	0	-14	87	0	0	231
11	Creep Check	"	4:15 p.m.	0	-14	87	29	0	231
12	Overnight Creep Check	8 June	8:30 a.m.	-14	-29	115	72	0	-72
13	Before 3rd Loading Increment	"	9:40 a.m.	-14	-43	101	87	0	-87
14	After 3rd Loading Increment	"	10:05 a.m.	-14	-43	101	101	0	-87
15	Before 4th Loading Increment	"	11:50 a.m.	-14	-29	101	-274	0	-72
16	After 4th Loading Increment	"	11:55 a.m.	-29	-58	72	-505	0	-43
17	Before 5th Loading Increment	"	2:50 p.m.	14	0	115	-29	29	245
18	After 5th Loading Increment	"	2:58 p.m.	14	0	128	-14	43	303
19	Before 6th Loading Increment	"	3:45 p.m.	14	0	128	-14	29	346
20	After 6th Loading Increment	"	3:55 p.m.	0	-29	115	0	29	360
21	Settled on Supports Overnight	9 June	8:30 a.m.	43	0	274	534	87	72
22	On Removal of Supports	"	9:30 a.m.	58	0	288	548	72	43
23	Before Unloading 6th Increment	"	2:30 p.m.	115	72	418	591	115	534
24	Before Unloading 5th Increment	"	2:35 p.m.	101	58	404	591	115	534
25	Before Unloading 4th Increment	"	2:40 p.m.	101	72	418	606	115	519
26	Before Unloading 3rd Increment	"	2:43 p.m.	101	101	447	606	115	505
27	Before Unloading 2nd Increment	"	2:46 p.m.	101	101	461	606	115	476
28	Before Unloading 1st Increment	"	2:49 p.m.	101	115	461	591	115	447
29	Fully Unloaded	"	2:53 p.m.	128	144	*	591	128	404
30	Permanent Set Check	"	3:21 p.m.	115	128	505	591	128	360

* For some unexplained reason, the printout from the data logger did not contain a reading here.

No. of Copies	To	No. of Copies	To
1	Office of the Director, Defense Research and Engineering, The Pentagon, Washington, D.C. 20301		Commander, Harry Diamond Laboratories, 2800 Powder Mill Road, Adelphi, Maryland 20783
12	Commander, Defense Documentation Center, Cameron Station, Building 5, 5010 Duke Street, Alexandria, Virginia 22314	1	ATTN: Technical Information Office
1	Metals and Ceramics Information Center, Battelle Columbus Laboratories, 505 King Avenue, Columbus, Ohio 43201		Commander, Picatinny Arsenal, Dover, New Jersey 07801
	Deputy Chief of Staff, Research, Development, and Acquisition, Headquarters Department of the Army, Washington, D. C. 20310	1	ATTN: Mr. A. M. Anzalone, Bldg. 3401
		1	Mr. J. Pearson
1	ATTN: DAMA-ARZ	1	G. Randers-Pehrson
		1	Mr. A. Devine
	Commander, Army Research Office, P. O. Box 12211, Research Triangle Park, North Carolina 27709	1	SARPA-RT-S
1	ATTN: Information Processing Office		Commander, Redstone Scientific Information Center, U. S. Army Missile Research and Development Command, Redstone Arsenal, Alabama 35809
1	Dr. F. W. Schmiedeshoff		
	Commander, U. S. Army Materiel Development and Readiness Command, 5001 Eisenhower Avenue, Alexandria, Virginia 22333	1	ATTN: DRDMI-TB
1	ATTN: DRCLDC, Mr. R. Zentner		Commander, Watervliet Arsenal, Watervliet, New York 12189
	Commander, U.S. Army Materiel Systems Analysis Activity, Aberdeen Proving Ground, Maryland 21005	1	ATTN: Dr. T. Davidson
		1	Mr. D. P. Kendall
1	ATTN: DRXSY-MP	1	Mr. J. F. Throop
	Commander, U. S. Army Communications Research and Development Command, Fort Monmouth, New Jersey 07703		Commander, U. S. Army Foreign Science and Technology Center, 220 7th Street, N. E., Charlottesville, Virginia 22901
1	ATTN: DRCDO-GG-TD	1	ATTN: Mr. Marley, Military Tech
1	DRCDO-GG-DM		Commander, U. S. Army Aeromedical Research Unit, P. O. Box 577, Fort Rucker, Alabama 36460
1	DRCDO-GG-E		
1	DRCDO-GG-EA	1	ATTN: Technical Library
1	DRCDO-GG-ES		Chief, Benet Weapons Laboratory, LCWSL, USA ARRADCOM, Watervliet Arsenal, Watervliet, New York 12189
1	DRCDO-GG-EG		
1	DRCDO-GG-EI	1	ATTN: DRDAR-LCB-TL
	Commander, U. S. Army Missile Research and Development Command, Redstone Arsenal, Alabama 35809		Director, Eustis Directorate, U. S. Army Air Mobility Research and Development Laboratory, Fort Eustis, Virginia 23604
1	ATTN: DRDMI-RKK, Mr. C. Martens, Bldg. 7120	1	ATTN: Mr. J. Robinson, DAVDL-E-MOS (AVRADCOM)
	Commander, U. S. Army Natick Research and Development Command, Natick, Massachusetts 01760	1	Mr. R. Berresford
1	ATTN: Technical Library		U. S. Army Aviation Training Library, Fort Rucker, Alabama 36360
1	Dr. E. W. Ross		
1	DRDNA-UE, Dr. L. A. McClaine	1	ATTN: Building 5906-5907
	Commander, U. S. Army Satellite Communications Agency, Fort Monmouth, New Jersey 07703		Commander, U. S. Army Agency for Aviation Safety, Fort Rucker, Alabama 36362
1	ATTN: Technical Document Center	1	ATTN: Librarian, Bldg. 4905
	Commander, U. S. Army Tank-Automotive Research and Development Command, Warren, Michigan 48090		Commander, USACDC Air Defense Agency, Fort Bliss, Texas 79916
1	ATTN: DRDTA-RKA	1	ATTN: Technical Library
1	DRDTA-UL, Technical Library		Commander, U. S. Army Engineer School, Fort Belvoir, Virginia 22060
	Commander, U. S. Army Armament Research and Development Command, Dover, New Jersey 07801	1	ATTN: Library
2	ATTN: Technical Library		Commander, U. S. Army Engineer Waterways Experiment Station, Vicksburg, Mississippi 39180
1	DRDAR-SCM, J. D. Corrie		
1	Dr. J. Fraiser	1	ATTN: Research Center Library
	Commander, White Sands Missile Range, New Mexico 88002		Commander, Naval Air Engineering Center, Lakehurst, New Jersey 08733
1	ATTN: STEWS-WS-VT	1	ATTN: Technical Library, Code 1115
	Commander, Aberdeen Proving Ground, Maryland 21005		Director, Structural Mechanics Research, Office of Naval Research, 800 North Quincy Street, Arlington, Virginia 22203
1	ATTN: STEAP-TL, Bldg. 305	1	ATTN: Dr. N. Perrone
	Commander, U. S. Army Armament Research and Development Command, Aberdeen Proving Ground, Maryland 21010		Naval Air Development Center, Aero Materials Department, Warminster, Pennsylvania 18974
1	ATTN: DRDAR-QAC-E	1	ATTN: J. Viglione
	Commander, U. S. Army Ballistic Research Laboratory, Aberdeen Proving Ground, Maryland 21005		David Taylor Naval Ship Research and Development Laboratory, Annapolis, Maryland 21402
1	ATTN: Dr. R. Vitali	1	ATTN: Dr. H. P. Chu
1	Dr. G. L. Filbey		Naval Underwater Systems Center, New London, Connecticut 06320
1	Dr. W. Gillich		
1	DRDAR-TSB-S (STINFO)	1	ATTN: R. Kasper
1	Mr. A. Elder		

No. of Copies	To
	Naval Research Laboratory, Washington, D.C. 20375
1	ATTN: C. D. Beachem, Head, Adv. Mat'ls Tech Br. (Code 6310)
1	Dr. J. M. Krafft - Code 8430
1	Dr. Jim C. I. Chang
	Chief of Naval Research, Arlington, Virginia 22217
1	ATTN: Code 471
	Naval Weapons Laboratory, Washington, D.C. 20390
1	ATTN: H. W. Romine, Mail Stop 103
1	Ship Research Committee, Maritime Transportation Research Board, National Research Council, 2101 Constitution Avenue, N. W., Washington, D.C. 20418
	Air Force Materials Laboratory, Wright-Patterson Air Force Base, Ohio 45433
2	ATTN: AFML (MXE), E. Morrissey
1	AFML (LC)
1	AFML (LLP), D. M. Forney, Jr.
1	AFML (LNC), T. J. Reinhart
1	AFML (MBC), Mr. Stanley Schulman
1	AFFDL (FB), Dr. J. C. Halpin
1	Dr. S. Tsai
1	Dr. N. Pagano
	Air Force Flight Dynamics Laboratory, Wright-Patterson Air Force Base, Ohio 45433
1	ATTN: AFFDL (FBS), C. Wallace
1	AFFDL (FBE), G. D. Sendeckyj
	National Aeronautics and Space Administration, Washington, D.C. 20546
1	ATTN: Mr. B. G. Achhammer
1	Mr. G. C. Deutsch - Code RW
	National Aeronautics and Space Administration, Marshall Space Flight Center, Huntsville, Alabama 35812
1	ATTN: R. J. Schwinghamer, EHO1, Dir., M&P Lab
1	Mr. W. A. Wilson, EH41, Bldg. 4612
	National Aeronautics and Space Administration, Langley Research Center, Hampton, Virginia 23665
1	ATTN: Mr. H. F. Hardrath, Mail Stop 188M
1	Mr. R. Foye, Mail Stop 188A
	National Aeronautics and Space Administration, Lewis Research Center, 21000 Brookpark Road, Cleveland, Ohio 44135
1	ATTN: Mr. S. S. Manson
1	Dr. J. E. Srawley, Mail Stop 105-1
1	Mr. W. F. Brown, Jr.
1	Mr. R. F. Lark, Mail Stop 49-3
	Panametrics, 221 Crescent Street, Waltham, Massachusetts 02154
1	ATTN: Mr. K. A. Fowler
	Wyman-Gordon Company, Worcester, Massachusetts 01601
1	ATTN: Technical Library
	Lockheed-Georgia Company, 86 South Cobb Drive, Marietta, Georgia 30063
1	ATTN: Materials & Processes Eng. Dept. 71-11, Zone 54
	National Bureau of Standards, U. S. Department of Commerce, Washington, D.C. 20234
1	ATTN: Mr. J. A. Bennett
1	Mechanical Properties Data Center, Belfour Stulen Inc., 13917 W. Bay Shore Drive, Traverse City, Michigan 49684
1	Mr. W. F. Anderson, Atomics International, Canoga Park, California 91303
1	Dr. J. Charles Grosskreutz, Asst. Dir. for Research, Solar Energy Research Institute, 1536 Cole Boulevard, Golden, Colorado 80401
1	Mr. A. Hurlich, Convair Div., General Dynamics Corp., Mail Zone 630-01, P. O. Box 80847, San Diego, California 92138

No. of Copies	To
	Virginia Polytechnic Institute and State University, Department of Engineering Mechanics, 230 Norris Hall, Blacksburg, Virginia 24061
1	ATTN: Prof. R. M. Barker
1	Assoc. Prof. G. W. Swift
	Southwest Research Institute, 8500 Culebra Road, San Antonio, Texas 78284
1	ATTN: Dr. P. Francis
1	Dr. W. Baker
	IIT Research Institute, Chicago, Illinois 60616
1	ATTN: Dr. I. M. Daniel
1	Mr. J. G. Kaufman, Alcoa Research Laboratories, New Kensington, Pennsylvania 15068
1	Mr. G. M. Orner, MANLABS, 21 Erie Street, Cambridge, Massachusetts 02139
1	Mr. P. N. Randall, TRW Systems Group - O-1/2210, One Space Park, Redondo Beach, California 90278
1	Dr. E. A. Steigerwald, TRW Metals Division, P. O. Box 250, Minerva, Ohio 44657
1	Dr. George R. Irwin, Department of Mechanical Engineering, University of Maryland, College Park, Maryland 20742
1	Mr. W. A. Van der Sluys, Research Center, Babcock and Wilcox, Alliance, Ohio 44601
1	Mr. B. M. Wundt, 2346 Shirl Lane, Schenectady, New York 12309
	Battelle Columbus Laboratories, 505 King Avenue, Columbus, Ohio 43201
1	ATTN: Mr. J. Campbell
1	Dr. E. Rybicki
1	Dr. K. R. Merckx, Battelle Northwest Institute, Richland, Washington 99352
	General Electric Company, Schenectady, New York 12010
1	ATTN: Mr. A. J. Brothers, Materials & Processes Laboratory
	General Electric Company, Knolls Atomic Power Laboratory, P. O. Box 1072, Schenectady, New York 12301
1	ATTN: Mr. F. J. Mehringer
1	Dr. L. F. Coffin, Room 1C41-K1, Corp. R&D, General Electric Company, P. O. Box 8, Schenectady, New York 12301
	United States Steel Corporation, Monroeville, Pennsylvania 15146
1	ATTN: Dr. A. K. Shoemaker, Research Laboratory, Mail Stop 78
	Westinghouse Electric Company, Bettis Atomic Power Laboratory, P. O. Box 109, West Mifflin, Pennsylvania 15122
1	ATTN: Mr. M. L. Parrish
	Westinghouse Research and Development Center, 1310 Beulah Road, Pittsburgh, Pennsylvania 15235
1	ATTN: Mr. E. T. Wessel
1	Mr. M. J. Manjoine
1	Dr. Alan S. Tetelman, Failure Analysis Associates, Suite 4, 11777 Mississippi Ave., Los Angeles, California 90025
	Brown University, Providence, Rhode Island 02912
1	ATTN: Prof. J. R. Rice
1	Prof. W. N. Findley, Division of Engineering, Box D
	Carnegie-Mellon University, Department of Mechanical Engineering, Schenley Park, Pittsburgh, Pennsylvania 15213
1	ATTN: Dr. J. L. Swedlow
1	Prof. J. D. Lubahn, Colorado School of Mines, Golden, Colorado 80401

No. of Copies	To
1	Prof. J. Dvorak, Civil Engineering Department, Duke University, Durham, North Carolina 27706
1	George Washington University, School of Engineering and Applied Sciences, Washington, D.C. 20052 ATTN: Dr. H. Liebowitz
1 1	Lehigh University, Bethlehem, Pennsylvania 18015 ATTN: Prof. G. C. Sih, Prof. F. Erodgan
1	Terra Tek, University Research Park, 420 Wakara Way, Salt Lake City, Utah 84108 ATTN: Dr. A. Jones
1	P. R. Mallory Company, Inc., 3029 East Washington Street, Indianapolis, Indiana 46206 ATTN: Technical Library
1	Librarian, Material Sciences Corporation, Blue Bell Office Campus, Merion Towle House, Blue Bell, Pennsylvania 19422
1 1 1 1	Massachusetts Institute of Technology, Cambridge, Massachusetts 02139 ATTN: Prof. F. A. McClintock, Room 1-304, Prof. T. H. H. Pian, Department of Aeronautics and Astronautics, Prof. F. J. McGarry, Prof. A. S. Argon, Room 1-306
1	Prof. J. N. Rossettos, Department of Mechanical Engineering, Northeastern University, Boston Massachusetts 02115
1	Prof. R. Greif, Department of Mechanical Engineering, Tufts University, Medford, Massachusetts 02155
1	Dr. D. E. Johnson, AVCO Systems Division, Wilmington, Massachusetts 01887
1 1	University of Delaware, Department of Aerospace and Mechanical Engineering, Newark, Delaware 19711 ATTN: Prof. B. Pipes, Prof. J. Vinson
1	Syracuse University, Department of Chemical Engineering and Metallurgy, 409 Link Hall, Syracuse, New York 13210 ATTN: Mr. H. W. Liu
1	Prof. W. Goldsmith, Department of Mechanical Engineering, University of California, Berkeley, California 94720
1	University of California, Los Alamos Scientific Laboratory, Los Alamos, New Mexico 87544 ATTN: Dr. R. Karpp

No. of Copies	To
1	Prof. A. J. McEvily, Metallurgy Department U-136, University of Connecticut, Storrs, Connecticut 06268
1	Prof. D. Drucker, Dean of School of Engineering, University of Illinois, Champaign, Illinois 61820
1 1	University of Illinois, Urbana, Illinois 61801 ATTN: Prof. H. T. Corten, Department of Theoretical and Applied Mechanics, 212 Talbot Laboratory, Dr. T. Lardner, Department of Theoretical and Applied Mechanics
1	Prof. R. I. Stephens, Materials Engineering Division, University of Iowa, Iowa City, Iowa 52242
1	Prof. D. K. Felbeck, Department of Mechanical Engineering, University of Michigan, 2046 East Engineering, Ann Arbor, Michigan 48109
1	Dr. M. L. Williams, Dean of Engineering, 240 Benedum Hall, University of Pittsburgh, Pittsburgh, Pennsylvania 15260
1	Prof. A. Kobayashi, Department of Mechanical Engineering, FU-10, University of Washington, Seattle, Washington 98195
1	Mr. W. A. Wood, Baillieu Laboratory, University of Melbourne, Melbourne, Australia
1	Mr. Elmer Wheeler, Airesearch Manufacturing Company, 402 W. 36th Street, Phoenix, Arizona 85034
1	Mr. Charles D. Roach, U. S. Army Scientific and Technical Information Team, 6000 Frankfurt/Main, I. G. Hochhaus, Room 750, West Germany (APO 09710, NY)
1	Prof. R. Jones, Department of Civil Engineering, Ohio State University, 206 W. 18th Avenue, Columbus, Ohio 43210
1	State University of New York at Stony Brook, Stony Brook, New York 11790 ATTN: Prof. Fu-Pen Chiang, Department of Mechanics
1	E. I. Du Pont de Nemours and Company, Wilmington, Delaware 19898 ATTN: Dr. Carl Zweben, Industrial Fibers Division, Textile Fibers Department
1	Lawrence Livermore Laboratory, Livermore, California 94550 ATTN: Dr. E. M. Wu
1	Denver Research Institute, 2390 South University Boulevard, Denver, Colorado 80210 ATTN: Dr. R. Recht
2 1 1	Director, Army Materials and Mechanics Research Center, Watertown, Massachusetts 02172 ATTN: DRXMR-PL, DRXMR-WD, Author